Compounds from an Unbiased Chemical Screen Reverse Both Er-to-Golgi Trafficking Defects and Mitochondrial Dysfunction in Parkinson's Disease Models

Compounds from an unbiased chemical screen reverse both ER-to-Golgi trafficking defects and mitochondrial dysfunction in Parkinson disease models

Linhui Julie Su[1,9,*], Pavan K. Auluck[1,3,*], Tiago Fleming Outeiro[1,10,*], Esti Yeger-Lotem[1,4,11], Joshua A. Kritzer[1,12], Daniel F. Tardiff[1], Katherine E. Strathearn[5], Fang Liu[5], Songsong Cao[6], Shusei Hamamichi[6], Kathryn J. Hill[7], Kim A. Caldwell[6], George W. Bell[1], Ernest Fraenkel[4], Antony A. Cooper[7], Guy A. Caldwell[6], J. Michael McCaffery[8], Jean-Christophe Rochet[5], and Susan Lindquist[1,2]

1. Whitehead Institute for Biomedical Research, Cambridge, MA 02142 USA
2. Howard Hughes Medical Institute, Cambridge, MA 02142 USA
3. Department of Pathology, Massachusetts General Hospital, Boston, MA 02114 and Harvard Medical School, Boston MA 02115 USA
4. Department of Biological Engineering, MIT, Cambridge, MA, 02142 USA
5. Department of Medicinal Chemistry and Molecular Pharmacology, Purdue University, West Lafayette, IN, 47907 USA
6. Department of Biological Sciences, University of Alabama, Tuscaloosa, AL, 35487 USA
7. Diabetes Program, Garvan Institute of Medical Research, Sydney, NSW 2010 Australia
8. Integrated Imaging Center, Department of Biology, Johns Hopkins University, Baltimore, MD 21218 USA
9. Present Address: Adnexus Therapeutics, A Bristol-Myers Squibb R&D Company, Waltham, MA 02453, USA
10. Present Address: Cell and Molecular Neuroscience Unit, Instituto de Medicina Molecular and Instituto de Fisiologia, Faculdade de Medicina da Universidade de Lisboa, Lisboa, Portugal
11. Present Address: Department of Clinical Biochemistry, Soroka Medical Center and the National Institute for Biotechnology in the Negev, Ben-Gurion University of the Negev, Beer-Sheva, 84105, Israel.
12. Present Address: Department of Chemistry, Tufts University, Medford, MA 02155, USA

* These authors contribute equally

Corresponding Author: Susan Lindquist
Whitehead Institute for Biomedical Research
9 Cambridge Center
Cambridge, MA 02142
E-mail: *lindquist_admin@wi.mit.edu*
Fax: 617-258-7226

Running Title: ER and mitochondrial dysfunction in PD
Key Words: α-synuclein, mitochondria, Parkinson
Word Count: 7730 Words
Abstract: 287 Words
Title: 128 Characters
Running Title: 33 Characters

Alpha synuclein (α-syn) is a small lipid binding protein involved in vesicle trafficking whose function is poorly characterized. It is of great interest to human biology and medicine because α-syn dysfunction is associated with several neurodegenerative disorders including Parkinson Disease (PD). We previously created a yeast model of α-syn pathobiology, which established vesicle trafficking as a process that was particularly sensitive to α-syn expression. We also uncovered a core of proteins with diverse activities related to α-syn toxicity conserved from yeast to mammalian neurons. Here we report that a yeast strain expressing a somewhat higher level of α-syn also exhibits strong defects in mitochondrial function. Unlike our earlier strain, genetic suppression of ER-to-Golgi trafficking alone does not suppress α-syn toxicity in this strain. In an effort to identify individual compounds that could simultaneously rescue these apparently disparate pathologic effects of α-syn, we screened a library of 115,000 compounds. Indeed, we identified a class of small molecules that reduced α-syn toxicity at micromolar concentrations in this higher toxicity strain. These compounds reduced the formation of α-syn foci, re-established endoplasmic reticulum (ER)-to-Golgi trafficking, and ameliorated α-syn mediated damage to mitochondria. They also corrected the toxicity of α-syn in nematode neurons and in primary rat neuronal midbrain cultures. Remarkably the compounds also protected neurons against rotenone-induced toxicity, which has been used to model the mitochondrial defects associated with PD in humans. That single compounds are capable of rescuing the diverse toxicities of α-syn in yeast and neurons suggests that they are acting on deeply rooted biological processes that connect these toxicities and have been conserved for a billion years of eukaryotic evolution. Thus, it seems possible to develop novel therapeutic strategies to simultaneously target the multiple pathological features of PD.

α-Synuclein (α-syn) dysfunction has a well-established association with several neurodegenerative diseases including Parkinson disease (PD), dementia with Lewy bodies (DLB), and Multiple Systems Atrophy (MSA). PD is characterized by the degeneration of dopaminergic (DA) neurons in the substantia nigra pars compacta (SNpc) and other

brainstem and cortical nuclei (Braak et al., 2003); DLB by widespread cortical neuronal loss; and MSA by neuronal loss in the brainstem, cerebral cortex, and cerebellum. Both PD and DLB feature the formation of Lewy bodies (LBs) and Lewy Neurites (LNs) which are proteinaceous cytoplasmic aggregates composed of α-synuclein (α-syn) (Spillantini et al., 1997). In MSA, on the other hand, α-syn accumulates as morphologically distinct cytoplasmic inclusions in both neurons and glia (Spillantini et al., 1998). Both missense mutations and amplification of α-syn (Polymeropoulos et al., 1997; Kruger et al., 1998; Singleton et al., 2003; Ibanez et al., 2009) are linked to dominantly inherited forms of PD and DLB and recent genome-wide-analyses have linked α-syn to idiopathic PD, DLB, and MSA (Farrer et al., 2001; Kay et al., 2008; Scholz et al., 2009). Thus, it is becoming increasingly clear that α-syn dysfunction is central to the pathogenesis of these diseases.

α-Syn is a small 14.5 kDa protein ubiquitously expressed in the brain capable of associating with membranes (Jo et al., 2000; Cole et al., 2002). Its function remains poorly understood. When not bound to lipids α-syn is natively unfolded and is prone to forming toxic oligomers and higher ordered aggregates (Cole et al., 2002). These simple biophysical properties make α-syn an attractive subject for study in yeast, where the protein homeostasis machinery, vesicle-trafficking pathways, and even lipid metabolism pathways are highly conserved (Outeiro and Lindquist, 2003; Cooper et al., 2006; Gitler et al., 2008).

Yeast has most well-characterized eukaryotic genome and is amenable to rapid genetic interrogation. To take advantage of yeast genetics in dissecting the biology of α-syn, we placed α-syn under the control of the galactose inducible promoter. This allows synchronous induction of the transgene in all cells in the culture upon a switching the carbon source from raffinose to galactose media. By varying the copy number and integration loci of α-syn we found an unusually strong dose-dependence between α-syn expression levels and toxicity (Cooper et al., 2006; Gitler et al., 2008), highly reminiscent of the extreme dosage sensitivity of α-syn observed with certain dominantly-inherited forms of PD (Singleton et al., 2003; Ibanez et al., 2009). In this model, α-syn toxicity causes lipid droplet accumulation (Outeiro and Lindquist, 2003), impairs proteasome-mediated protein degradation (Chen et al., 2005; Sharma et al., 2006), and elicits vesicle trafficking defects (Outeiro and Lindquist, 2003; Soper et al., 2008) with specific ER-to-

Golgi blockade (Cooper et al., 2006; Gitler et al., 2008). All of these phenotypes have been observed in neuronal models and implicated in the pathogenesis of PD. Specifically, proteasomal impairment results in increased levels of α-syn in patient-derived fibroblasts (Hoepken et al., 2008) and the formation of fibrillar α-syn inclusions in primary rat neurons (Rideout et al., 2004); lipid droplets can promote the oligomerization of α-syn (Cole et al., 2002) and are associated with Lewy bodies in PD brains (Gai et al., 2000), and deletion of α-syn results in depletion of presynaptic vesicle pools (Abeliovich et al., 2000; Murphy et al., 2000; Cabin et al., 2002).

The extreme dosage sensitivity of α-syn allowed us to construct a modestly toxic α-syn strain (IntTox) which enabled a high-throughput unbiased genetic screen to identify *both* enhancers *and* suppressors of α-syn toxicity (Cooper et al., 2006; Yeger-Lotem et al., 2009). This screen identified genes involved in ER-to-Golgi trafficking (Cooper et al., 2006; Gitler et al., 2008), nitrosative stress, oxidative stress, and manganese transport (Yeger-Lotem et al., 2009). Human homologues of eight of these yeast genes (including *PARK9/ATP13A2*, a lysosomal ATPase; *PLK2*, a Polo-like kinase; and *SYVN1*, an E3 ubiquitin ligase) were tested in other models of PD and seven were confirmed to modify α-syn toxicity in neurons (Cooper et al., 2006; Gitler et al., 2008; Gitler et al., 2009; Yeger-Lotem et al., 2009). Thus the yeast work revealed that α-syn is part of a diverse genetic interactome that is conserved from yeast to mammals. Further, we identified *YPK9*, the yeast homolog of *PARK9/ATP13A2*, as a suppressor of α-syn toxicity in our genetic screen. Mutations in this gene are associated with autosomal-recessive Parkinsonism with dementia and pallidopyramidal degeneration (Kufor-Rakeb syndrome; OMIM 606693), but there had previously been no link between this disease and α-syn. In yeast, *YPK9* helped to alleviate manganese toxicity and restored α-syn localization to the membrane. The disease-associated mutations eliminated these functions when introduced into the Ypk9 protein. These results establish that the core biological processes affected by α-syn have been conserved across eukaryotic evolution and demonstrate the utility of yeast in investigating its biology and pathobiology.

Here we investigated a yeast strain that expresses higher levels of α-syn (HiTox) than the strain used in our earlier genetic screens (IntTox) (Cooper et al., 2006; Gitler et al., 2009; Yeger-Lotem et al., 2009). In various experiments using ELISA assays, the

expression level of α-syn in HiTox cells was 1.4 to 2.5 fold of the α-syn expression level in the IntTox cells. One striking difference between these two strains is that most of the genetic modifiers which strongly suppress α-syn toxicity in the IntTox strain do not effectively suppress toxicity in the HiTox strain on their own (Gitler et al., 2009; Kritzer et al., 2009). Instead, co-expression of two suppressors from diverse pathways is required to restore viability in the HiTox strain. This suggests that multiple pathways are being affected by α-syn in this strain. We turned to transcriptional profiling to elucidate these complex biological responses to α-syn and performed a high throughput chemical screen to determine if it was possible to discover individual compounds that could rescue diverse aspects of α-syn toxicity.

RESULTS

Transcriptional profiling reveals mitochondrial stress as an early signature of α-syn toxicity

We compared the transcriptional profile of HiTox cells with that of cells transformed with the vector alone (Vector) and with cells expressing a non-toxic low-expression level of α-syn (NoTox) (Fig. 1A, Tables S1 and S2). At non-toxic levels, α-syn expression elicited only a minimal transcriptional response that was slightly enriched for genes regulating carbon metabolism (Fig. 1B and Table S1). The HiTox α-syn strain, however, elicited a marked transcriptional response as early as two hours after induction, before any dying cells can be detected (Fig. 1A). This response markedly intensified after four hours of induction (Fig. 1A, Table S2) when only a few cells in the culture were starting to die (Cooper et al., 2006; Gitler et al., 2008) (Fig. S1).

Our analysis, using the gene ontology (GO) annotation of differentially regulated genes (Hong et al., 2008; Barrell et al., 2009) showed global down-regulation in the expression of ribosomal genes (28% [% of all genes with transcriptional changes], $p<10^{-30}$) (Fig. 1B, Table S2). This was one of the earliest changes detected. However, it is a common signature of just about any stressful condition in yeast (Gasch et al., 2000) and is not particularly informative regarding α-syn toxicity.

Other transcriptional changes were more specific to α-syn toxicity. At the earliest time point, just two hours after induction, we found marked decreases in transcripts

involved in the function and maintenance of the mitochondria (Fig. 1B). After two additional hours of induction, the down-regulation of mitochondrial and respiratory transcripts was much more pronounced (60%, $p<10^{-44}$) (Fig. 1B). This finding was particularly striking given that only two mitochondrial genes were identified as modifiers of the α-syn IntTox strain (Cooper et al., 2006; Yeger-Lotem et al., 2009). One was the suppressor *Hap4*, a transcriptional activator of respiratory genes (De Winde and Grivell, 1995). The other, *Mks1*, enhanced α-syn toxicity. Mks1 is a negative regulator of the retrograde signaling pathway. This pathway senses mitochondrial dysfunction and evokes a nuclear transcriptional response (Liu et al., 2003). Hence in the IntTox strain, this pathway appears to be acting to alleviate mitochondrial dysfunction caused by α-syn. Presumably, in the HiTox strain, the capacity of this pathway to counteract the toxicity of α-syn is overwhelmed.

In addition to this alteration in mitochondrial transcripts, we found that transcripts for genes with oxidoreductase activities were increased at 2 and 4 hours of induction (13%, $p<10^{-9}$) (Fig. 1B). This set of oxidoreductase genes was previously reported to increase in response to oxidative, osmotic, or aldehyde stress (Attfield, 1997). Together with the mitochondrial signature, we hypothesize that mitochondrial dysfunction is associated with oxidative stress in the HiTox strain.

α-Syn toxicity results in mitochondrial dysfunction and the generation of reactive oxygen species

To investigate the implications of these transcriptional alterations, we turned to thin-section ultrastructural electron microscopy (EM) to examine mitochondrial morphology. As we have previously reported, the IntTox strain exhibited a striking accumulation and clustering of vesicles, both at the periphery and interior of the cells (Gitler et al., 2008), and accumulation of lipid droplets in the cytoplasm (Outeiro and Lindquist, 2003). These changes also occurred in the HiTox strain. But in addition we observed hypertrophy of the ER with invagination of the ER membranes and mislocalization from the periphery of the cell to interior (Fig. 2A, c, inset).

Mitochondria in the HiTox α-syn cells were also markedly abnormal. Healthy mitochondria are typically compact with stacked, hyperintense mitochondrial membranes

(Fig. 2A, a and b) (Vander Heiden et al., 1997). Instead of retaining their typical ribbon-like architecture, the mitochondria of HiTox cells were swollen and circular with isointense electron-density with respect to the cytoplasm (Fig. 2A, c). These morphological changes correlate closely with loss of mitochondrial membrane potential and are indicative of dysfunctional mitochondria (Vander Heiden et al., 1997). Mitochondrial changes were only rarely observed in the IntTox strain (data not shown) (Gitler et al., 2008).

Given the relationship between mitochondrial dysfunction and reactive oxygen species (ROS) in PD (Foley and Riederer, 2000; Abou-Sleiman et al., 2006), we assayed for the production of ROS with 5-(and-6)-chloromethyl-2´, 7´-dichlorodihydrofluorescein diacetate (CM-H_2DCFDA), a cell permeable compound that fluoresces green upon oxidation by specific ROS (peroxynitrite, OH•, and H_2O_2). As expected, ROS was detected in fewer than 3% of vector, NoTox, or IntTox α-syn cells (Fig. 2B and data not shown). HiTox α-syn cells, however, exhibited a marked amount of ROS with over 30% of cells showing fluorescence with treated with CM-H_2DCFDA (Fig. 2B). Together with the ultrastructural mitochondrial changes, the generation of ROS suggests that high-levels of α-syn elicit global mitochondrial dysfunction.

Mitochondrial toxicity is not associated with mitochondrial localization of α-syn

Recent studies have suggested that α-syn may localize to mitochondria (Cole et al., 2008; Devi et al., 2008; Parihar et al., 2008). In our previous studies using immunogold electron microscopy, we did not find localization of α-syn to mitochondria in yeast (Gitler et al., 2008). However, these studies had employed the IntTox strain which has much less mitochondrial damage. Therefore, we revisited this issue asking whether, in the HiTox yeast strain, α-syn elicited mitochondrial damage by mislocalizing to the mitochondria. We employed a more quantitative method, differential centrifugation, to isolate distinct cellular compartments. This technique allows for the detection of even small quantities of α-syn. The purity of individual fractions was confirmed with compartment-specific markers (protein disulfide isomerase for ER, porin for mitochondria, alkaline phosphatase for vacuole, and phosphoglycerate kinase for cytosol; Fig. 2C).

We then probed for α-syn in each compartment and found that less than 0.2% of total α-syn was present in the mitochondrial fraction (Fig. 2C); most of the α-syn was

found in the soluble fraction with a smaller amount separating with the ER and vacuole (Fig 2C). The small amount of α-syn identified in the mitochondrial fraction likely represents minor contamination from other cellular compartments (note for example a similar level of reactivity with antibodies against alkaline phosphatase, a vacuolar marker, was also observed; Fig. 2C). Importantly, on long exposure, there was no increase in the small fraction of α-syn in the mitochondrial fraction in HiTox cells relative to cells expressing low, completely non-toxic levels of α-syn. Thus mitochondrial dysfunction elicited by α-syn is not due to specific mislocalization to mitochondria through a cryptic signaling sequence. Rather, it is the perturbation of other cellular pathways impinged on by α-syn that leads to mitochondrial dysfunction and the generation of reactive free radicals.

A high throughput chemical screen identifies strong suppressors of α-syn toxicity.

We next used this HiTox α-syn strain in a high-throughput chemical screen to identify single agents that might be capable of rescuing the robust toxicity of this strain. We hoped that identifying such a compound would uncover deeply-rooted aspects of α-syn biology linking the disparate pathologic phenotypes associated with toxicity. The multiple toxic phenotypes of this strain also created such a high level of stringency that we anticipated recovering only a small number of compounds that could reproducibly suppress α-syn toxicity. To score positive in the screen, the compounds needed to be able to 1) enter cells, 2) avoid clearance by core metabolic pathways, 3) alleviate α-syn toxicity without causing toxicity on their own at the screening concentration (Fleming et al., 2008) and 4) protect against at least two different features of α-syn toxicity within the HiTox cells (Gitler et al., 2009).

A library of 115,000 small compounds was screened at a concentration of 17 μg/ml (~ 15 μM) for the ability to ameliorate HiTox α-syn toxicity. Our initial compound hits were subsequently tested at lower concentrations (0.1 – 10 μM) to identify the most potent molecules capable of rescuing the HiTox α-syn cells (data not shown). Although none of the compounds completely restored normal growth, a few restored cell growth to ~50% of the density of wild-type cells after 48 hours of growth in galactose media (data not shown). Four 1,2,3,4-tetrahydroquinolinones denoted (**1**), (**2**), (**3**), and (**4**) (Fig. 3A, B) satisfied

these stringent criteria: these compounds were effective at low micromolar concentrations; exhibited significant dose-dependent rescue of growth; and were not toxic to wildtype cells (Fig. S2). By quantifying the growth rate between 5 and 10 hours, we determined that compound (**3**) was the most potent at the lowest concentrations, compounds (**2**) and (**4**) were equally potent at higher concentrations, and that compound (**1**) exhibited only weak protective activity at all concentrations tested (Fig. 3C). These compounds also demonstrated robust protective activity in a flow cytometric assay for cell death (Fig. 3D), with the most effective compound (compound (**3**), Fig. 3C) reducing α-syn-induced cell death from ~25% to 10% after six hours of α-syn expression (Fig. 3D).

We next asked if the compounds simply reduced the expression of α-syn from the galactose promoter. By western blotting, there was no measurable reduction on the amount of α-syn (data not shown). However, the strong dosage sensitivity of α-syn raised the possibility that even a slight alteration of expression could potentially alter the toxic phenotype. To further exclude potential transcriptional or promoter effects, we examined the efficacy of the compounds against α-syn toxicity when gene expression was controlled using an estradiol-inducible transcriptional trans-activator (Louvion et al., 1993). Under these conditions, the compounds were still protective against α-syn toxicity thereby excluding the possibility that suppression was simply the result of reduced induction from the galactose promoter (Fig. S3).

We also tested the compounds in a yeast model for Huntington disease (Duennwald et al., 2006) to determine whether these compounds were general modifiers of cellular toxicity or if they addressed specific pathologic processes unique to α-syn. None of the compounds restored growth in yeast expressing a toxic huntingtin fragment bearing a polyglutamine expansion (Fig. S4). Thus the compounds are not simply generalized modulators of cell stress.

To address whether the compounds altered the oligomerization properties of α-syn, we examined the compounds' ability to alter the fibrillization of α-syn using a thioflavin-T fluorescence assay. Monomeric wildtype α-syn was incubated at 25ºC with slight agitation in the presence of thioflavin-T which emits at 490 nm only when bound to amyloid fibrils. We found that the compounds had no effect on the rate of conformational transitions of α-

syn from monomer to amyloid fibers (Fig. S5), suggesting that they do not interact directly with α-syn.

We also identified two commercially available, structurally related 1,2,3,4-tetrahydroquinolinones that differed from the original compounds only by the functional groups appended to the phenyl ring (Fig. 3A; compounds (**5**) and (**6**)). These related compounds did not rescue the growth of HiTox α-syn cells at any concentration tested (Figs 3A, C, D and S3).

Compounds identified in the yeast screen also rescue α-syn-mediated dopaminergic neuron loss in a nematode model of PD.

Before pursuing detailed investigations characterizing the compounds, we sought to determine whether they were also effective in neuronal models of PD. First, we tested a *C. elegans* model expressing wild-type α-syn in DA neurons (Cao et al., 2005; Cooper et al., 2006). In this model, dopaminergic neurons remain in their proper neuroanatomical context. Because development is highly stereotyped in nematodes, wild-type animals always have exactly the same number of DA neurons. Directed expression of α-syn by the dopamine transporter promoter (P_{dat-1}) results in a highly reproducible age-dependent loss of DA neurons in ~50% of animals within 172 hours of age (neurons were scored for both intact cell bodies and preservation of neuritic processes) (Cao et al., 2005).

As free-living soil organisms, nematodes have thick cuticles and strong drug efflux pumps which necessitated that we first test their ability to tolerate 1% DMSO, the vehicle in which our compounds were administered. Under these conditions, neither the compounds nor 1% DMSO itself, exerted any toxic effect on wildtype worms not expressing α-syn. Newly hatched embryos expressing α-syn were able to tolerate 1% DMSO for up to 24 hours and two-day-old adult worms tolerated 1% DMSO for 8 hours with no additional neuronal loss (data not shown). Remarkably, the exposure of newly hatched embryos to ~ 15 μM of compounds (**1**), (**3**), and (**4**) in 1 % DMSO for just 24 hours achieved a substantial rescue of α-syn toxicity. After aging worms for an additional 148 hours after removal of the compounds, the percentage of worms with a full complement of neurons was increased to 70% from 50% (Fig. 4A & C). Moreover, two-day-old adult worms that were treated with compound (**1**) for only 8 hours also retained

more DA neurons and dendritic connections (Fig. 4B). Subtler but statistically significant neuroprotective effects were observed with compounds (**2**), (**3**) and (**4**), but not (**5**) and (**6**). It is remarkable that brief treatment of adult worms with these compounds was neuroprotective well after the onset of α-syn expression, revealing that it is possible to arrest cell death even after the onset of toxicity.

Rescue of α-syn-mediated dopaminergic neurotoxicity in mammalian cells.

We next sought to test the efficacy of these compounds in a mammalian model of PD. Stage 17 embryos were harvested from pregnant rats and their midbrains were carefully dissected, gently dissociated, and cultured in vitro for seven days. They were then transduced for 72 hours with a lentivirus encoding a mutant form of α-syn that is associated with autosomal-dominant PD (A53T). This well-established PD model (Liu et al., 2008a), while labor intensive, provides a robust and more reproducible measure of toxicity than we have been able to attain with any stable cell lines. This may be because the cultures recapitulate natural interactions between glia and neurons and/or because the cell lines have lost apoptotic mechanisms during immortalization and transformation. An additional benefit of this system is that lentiviral transfection is not restricted to a particular cell type and thus allows for the assessment of the preferential toxicity and rescue of DA neurons relative to other neurons in the culture.

Transduction of rat midbrain cultures with lentivirus encoding α-syn-A53T elicited a reduction in the total number of neurons (MAP2-positive neurons) and GABAergic neurons (GABA-positive neurons) within 96 hours (Liu et al., 2008a) (Fig. 4D). Notably, these neurons featured marked retraction of their processes (Fig. 4D). Although few tyrosine hydroxylase (TH)-positive neurons are present in individual microscopic fields, quantification of many fields revealed that the reduction in their numbers of these neurons was even more dramatic (Fig. 4E) (Cooper et al., 2006; Liu et al., 2008a). Remarkably, treatment with (**1**), (**2**), and (**3**), but not with vehicle, yielded a robust increase in the relative number of TH+ positive neurons (Fig. 4E), and substantially prevented the aberrant morphologies of the surviving neurons (Fig. 4D). Treated neurons, including TH-positive neurons, retained their complex branched dendritic arborization (Fig. 4D). Intriguingly, while compound (**4**) was not effective, compound (**6**), which had been

inactive in both yeast and C. elegans, exhibited a protective effect in this neuronal assay (Fig. 4E).

Structure-activity relationships uncover only minor differences among models in three different organisms

It is important to note that compounds (**3**), (**4**) and (**6**) are structurally very similar and differ only in the functional groups appended to the phenyl group (Fig. 3A). This structural similarity suggested that the compounds might interact with the same target. Indeed, when we performed competition assays in HiTox yeast cells, by mixing the most effective compound (**3**) with increasing concentrations of the yeast-inactive compounds (**5**) or (**6**), they strongly interfered with rescue by compound (**3**) (Fig. S2 and data not shown). Further, transcriptional analysis of the compounds in yeast revealed that compounds (**5**) and (**6**) did have some, albeit limited, effects on reversing the transcriptional profile of HiTox α-syn (Fig. 1C, see below). Compounds (**5**) and (**6**) must therefore bind to the same target as compound (**3**), but simply do not affect its function appreciably. Thus, the bioactive compounds we identified in the yeast screen must act on a conserved target(s) that exhibits only minor differences in SAR over astonishing evolutionary distances.

Chemical suppressors of α-syn toxicity reverse mitochondrial abnormalities, reduce ROS production, and restore ER-to-Golgi trafficking.

Given the diversity of pathologic phenotypes present in the HiTox α-syn cells, we asked which were being reversed by these compounds. Transcriptional profiling of wild-type yeast cells revealed that the compounds elicited a negligible transcriptional response on their own, consistent with our finding that the compounds had no effect on the growth or viability of wildtype cells (Table S4). In HiTox α-syn cells, the active compounds had a profound effect on the transcriptional changes due to α-syn toxicity. Compounds (**1**) and (**2**) markedly reversed many of the transcriptional changes induced by high levels of α-syn (Fig. 1C). Compound (**4**) showed a more modest, yet similar effect on the transcriptional changes of HiTox cells (Fig. 1C) [correlation between profiles of cells treated with (**1**) and (**4**), r=0.74); differential findings among several replicates limited statistical analysis of transcripts from cells treated with (**3**)]. In contrast, the yeast inactive compounds (**5**) and

(**6**) yielded only a partial reduction in the transcriptional changes induced by HiTox α-syn (Fig. 1C). Overall, treatment with (**5**) or (**6**) correlated most closely with untreated HiTox cells ($r>0.86$).

Notably, the reversal in α-syn associated transcriptional changes was incomplete [$r=0.59$ for untreated vs. (**1**); $r=0.54$ for untreated vs. (**2**)]. Specifically, in HiTox cells treated with (**1**) or (**2**), the differentially regulated genes were still enriched for mitochondria-localized proteins (29%, $p<10^{-11}$), however the magnitude by which the expression of these genes changed was reduced in comparison to untreated cells (Fig. 1B and C). Genes involved in transition metal ion homeostasis (6%, $p<10^{-12}$) that increase in response to α-syn remained upregulated. Overall, the transcriptional profiles of HiTox cells treated with compounds revealed broad reductions in ER, mitochondrial, membrane, and oxidative stress pathways (Fig. 1C). Thus the compounds appear to be acting on a central core pathway that is either upstream of these pathways, or unites them.

Next we examined the effects of the compounds on the generation of ROS, ER-to-Golgi vesicle trafficking, and mitochondrial morphology. All of the active compounds caused a dramatic reduction in the generation of ROS in HiTox α-syn cells (Fig. 2B). The production of ROS in HiTox cells was completely restored to control levels by treatment with compound (**3**) but not with compound (**5**) (Fig. 2B). This finding raised the possibility that the compounds were cytoprotective by acting as scavengers of free radicals. We therefore tested several strong antioxidants for their ability to suppress α-syn toxicity. The antioxidants N-acetylcysteine, riboflavin and melatonin all protected against the toxicity of hydrogen peroxide to yeast cells (Figs S7-S9). In contrast, compound (**3**) did not rescue against hydrogen peroxide-induced toxicity (Fig. S7). None of the antioxidants protected against the cellular toxicity of α-syn in yeast (Figs S7-S9). Similarly these antioxidants did not protect against the toxicity of α-syn in the nematode or rat midbrain neuronal culture models (Figs S10 and S11) (Liu et al., 2008b). Thus rescue of toxicity by these compounds is not due to simple antioxidant activity.

ER-to-Golgi vesicle trafficking blockade is a significant component of α-syn toxicity in IntTox cells (Cooper et al., 2006) and is effectively rescued by the coexpression of Rab GTPases (Cooper et al., 2006; Gitler et al., 2008s06). This ER-to-Golgi block is associated with the mislocalization of α-syn from the plasma membrane to large foci

within both IntTox and HiTox cells (Outeiro and Lindquist, 2003; Cooper et al., 2006) but not in NoTox cells. The Rab proteins are largely ineffectual in protecting HiTox cells on their own (Gitler et al., 2009). They do so only when combined with genetic suppressors of different functional classes (Gitler et al., 2009; Kritzer et al., 2009). We found that, unlike the Rab proteins, all four bioactive compounds restored α-syn localization to the plasma membrane on their own in HiTox cells (Fig. 5A).

To specifically and quantitatively assay ER-to-Golgi trafficking, we measured the compartment-specific modifications acquired by carboxypeptidase Y (CPY) as it traverses from the ER to the Golgi to the vacuole. In healthy wild-type cells, less than 5% of CPY is retained in the ER 20 minutes after pulse with radiolabeled CPY (Cooper et al., 2006). In untreated HiTox cells that had been induced for 4.5 hours prior to pulse-labeling, 55% of CPY was retained in the ER after the 20 minute chase. This is similar to the ER-to-Golgi trafficking block we previously reported for the IntTox α-syn strain (Cooper et al., 2006). HiTox cells treated with vehicle or with the inactive compounds (**5**) and (**6**) exhibited a similar decrease in CPY trafficking (Fig. 5B). Remarkably, treatment with compounds (**1**), (**2**), (**3**), or (**4**) restored CPY trafficking to wildtype levels with only 5% retention in the ER (Fig. 5B).

Finally, to confirm the effects of the compounds on these diverse pathways, we examined HiTox cells by electron microscopy. HiTox cells treated with compound (**1**) – (**4**) still contained some swollen and isointense mitochondria, however, the frequency of these mitochondrial abnormalities was reduced (Fig. 5C). In addition, the active compounds largely restored ER localization to the periphery of the cells and reduced the size and number of vesicle clusters within HiTox cells (Fig. 5C, a-d). In contrast, none of these abnormalities were reversed upon treatment with either compound (**5**) or (**6**) (Fig. 5C, e & f). The fact that these compounds restored trafficking of CPY from the ER to Golgi in addition to reducing ROS production and restoring mitochondrial morphology demonstrates that it is possible to ameliorate several diverse cellular pathologies associated with PD with a single chemical agent.

Suppression of rotenone toxicity in mammalian dopaminergic neurons

Because the compounds reversed several different pathological phenotypes mediated by α-syn in yeast suggested that they might also protect mammalian cells from other sources of PD-related damage. Rotenone, a potent mitochondrial complex I inhibitor, is commonly used to elicit mitochondrial dysfunction, oxidative stress, and dopaminergic degeneration in mammalian systems. In cultured cells, it is considered a good model of the PD-related damage associated with mitochondrial toxins (Ayala et al., 2007).

As expected, exposure of primary rat midbrain cultures to 100 nM rotenone caused a robust decrease in the overall number of GABA+, MAP2+ and TH+ neurons. Rotenone also elicited marked morphological changes including retracted neuronal processes and shriveled neuronal somata (Fig. 6). As observed with α-syn-A53T transfection, TH+ neurons were lost in greater degree than other neurons (Fig. 6). Treatment with compounds (**1**) or (**4**) greatly abrogated the toxicity of rotenone in a dose-dependent manner and restored normal neuronal architecture (Figs 6 and S6). Compounds (**3**) and (**5**) also showed a trend towards neuroprotection, though results with (**3**) did not reach statistical significance (Fig. S6).

As previously reported, over-expression of Rab1 suppresses α-syn toxicity in yeast (the IntTox strain) by restoring ER-to-Golgi transport. It also rescues α-syn toxicity in *C. elegans, Drosophila melanogaster*, and rat neuronal cultures (Cooper et al., 2006). However, Rab1 did not reverse the toxicity of rotenone (Fig. S6). Thus, it appears that mitochondrial dysfunction is not a direct consequence of ER-to-Golgi trafficking defects alone, but of some other, closely related pathway affected by α-syn. The compounds must be acting on a target proximal to both pathways to be able to protect against high levels of α-syn toxicity in yeast and both α-syn and rotenone toxicity in mammalian cells.

Discussion

Our findings reveal deep links between distinct pathogenic aspects of α-syn toxicity. Our previous work demonstrated that ER-to-Golgi trafficking defects are a prominent feature of intermediate levels of α-syn toxicity in yeast (IntTox strain) and in higher organisms (Cooper et al., 2006). The IntTox strain also can be suppressed by single genetic modifiers (Yeger-Lotem et al., 2009). In contrast, the HiTox α-syn strain, which

only expresses ~50% more α-syn, requires two genetic suppressors acting in separate pathways to rescue growth (Gitler et al., 2009; Kritzer et al., 2009). Transcriptional profiling revealed that in this strain, in addition to ER-to-Golgi trafficking defects, mitochondrial dysfunction is an early pathologic phenotype. Mitochondrial dysfunction, which was associated with the generation of ROS and marked mitochondrial morphological changes, was not a feature of the previously described IntTox strain. Thus, the HiTox strain presented an opportunity to search for other core cellular processes affected by α-syn toxicity.

The identification of mitochondrial dysfunction and ROS as a consequence of higher levels of α-syn toxicity in yeast cells is extremely compelling given the wealth of evidence that link mitochondrial dysfunction and oxidative stress to PD [for review, see (Mandemakers et al., 2007)]. Humans accidentally exposed to the mitochondrial toxin 1-methyl-4-phenyl-1,2,3,6-tetrahydropyridine (MPTP) develop Parkinsonism resulting from the immediate loss of dopaminergic neurons in the substantia nigra (Davis et al., 1979; Langston et al., 1983). Similarly, rotenone induces dopaminergic degeneration with the accumulation of α-syn into LB-like aggregates when administered chronically to rats (Betarbet et al., 2000; Sherer et al., 2003; Norris et al., 2007). In cell culture and in vivo α-syn overexpression sensitizes both cells and mice to MPTP (Song et al., 2004; Smith et al., 2005). Moreover, aged transgenic mice over-expressing mutant α-syn exhibit profound mitochondrial defects within their neurons (Martin et al., 2006; Stichel et al., 2007) and mice lacking α-syn have increased resistance to mitochondrial toxins (Dauer et al., 2002; Drolet et al., 2004; Klivenyi et al., 2006) and alterations in mitochondrial lipid content (Ellis et al., 2005). Overall, despite a decade of intense investigation, a direct connection between α-syn toxicity and mitochondrial dysfunction has remained elusive.

Recent reports have suggested the existence of a cryptic mitochondrial targeting sequence within the amino terminal of α-syn (Cole et al., 2008; Devi et al., 2008; Parihar et al., 2008) that might be responsible for toxicity in this organelle. While we cannot exclude the possibility that α-syn might interact with mitochondria in mammalian cells, we found that only a very tiny fraction of α-syn localizes to mitochondria in the HiTox yeast cells which nevertheless exhibit profound mitochondrial defects (Fig. 2C). Furthermore, the same quantity of α-syn was detected in mitochondria of the NoTox strain indicating that

the localization of small quantities of α-syn to mitochondria is not responsible for toxicity. Yet, the mitochondrial toxicity we detect in yeast must be highly related to that caused by α-syn and rotenone in neurons because compounds selected to rescue yeast from α-syn also rescue neurons from both α-syn and rotenone. Rather that affecting mitochondria through direct localization to that organelle, our data indicate that α-syn interferes with deeply rooted biological processes that impinges upon pathways linking vesicle trafficking, the ER and mitochondria.

How might ER-to-Golgi trafficking defects and mitochondrial dysfunction be linked? Our earlier work has shown that the block in ER-to-Golgi trafficking is associated with impairment of ER-derived secretory vesicles failing to fuse with the Golgi (Gitler et al., 2008). Increased α-syn expression could exacerbate ER homeostasis defects which in turn could impact mitochondria in at least three different ways. The first derives from recent work demonstrating that mitochondria are focally tethered to the ER in both yeast (Kornmann et al., 2009) and mammalian cells (de Brito and Scorrano, 2008). This attachment allows mitochondria to sense and take-up Ca^{2+} released by the ER into the cytosol (de Brito and Scorrano, 2008). In addition to serving as a buffer for excess Ca^{2+}, Ca^{2+}-sensing also allows mitochondria to localize to parts of the cell (i.e. the synapse) where the local energy requirements are high. Thus, decoupling connections to the ER would impair the mitochondria's ability to sense and respond to cellular energy demands.

Second, a blockade in ER trafficking might disrupt the autophagic destruction of abnormal mitochondria, so-called "mitophagy" (Van Laar and Berman, 2009). The accumulation of dysfunctional mitochondria would then exacerbate cellular toxicity through the generation of ROS and impaired metabolism. Indeed, in both mammalian neurons and yeast, ROS are a salient feature of α-syn toxicity. The resultant ROS might also potentiate neurotoxicity by promoting the oligomerization of α-syn (Norris et al., 2003) thus creating a vicious toxic circle.

Finally, the ER and mitochondria also act together to coordinate lipid synthesis (Daum and Vance, 1997; Kornmann et al., 2009). Specifically, after phosphatidylserine is synthesized in the ER, it is transferred to mitochondria for decarboxylation by Psd1 after which it is shuttled back to the ER for subsequent modification to form phosphatidylcholine (Kornmann et al., 2009). α-Syn may impede the flow of biosynthetic

components between these organelles just as it impedes the flow of vesicles from ER to Golgi. Strikingly, abnormalities in lipid metabolism have also been noted in our yeast model (Outeiro and Lindquist, 2003) as well as in human PD brains (Gai et al., 2000). The application of high throughput genomic, proteomic, and lipidomic assays to our yeast model offers an opportunity for elucidating the vitally important connections between α-syn, the ER and mitochondria.

Our results also suggest reasons why neurons might be particularly sensitive to α-syn dysfunction. Compared to most cell types, neurons have unusually strong demands for vesicle trafficking. Catecholaminergic neurons are particularly susceptible because catecholamines are synthesized in the cytoplasm where they can exert toxicity unless they are immediately sequestered into secretory vesicles (Mosharov et al., 2009). Deficits in the production of secretory vesicles would therefore be particularly toxic to certain neuronal populations. Neurons also have intrinsically higher levels of respiration than most other cell types (Kandel, 2000) and are therefore vulnerable to disturbances in mitochondrial activity that are caused by α-syn. Finally, the transcriptional response of yeast cells to α-syn also revealed disruption of metal ion homeostasis (Fig. 1B). This corroborates our previous finding that three metal ion transporters (for manganese, Ca^{2+} and iron) modify α-syn toxicity (Gitler et al., 2009). The brain is also particularly sensitive to perturbations in the balance of these ions. Thus, the defects caused by α-syn would logically create a special combination of vulnerabilities in certain neurons.

Our unbiased chemical screen of 115,000 compounds against the HiTox α-syn strain identified compounds capable of protecting against multiple pathologic processes elicited by α-syn toxicity. The ability of these compounds to rescue disparate toxicities in this strain and to rescue both α-syn and rotenone toxicity in mammalian cells is remarkable. The efficacy of the compounds in neuronal models reveals that not only have the cellular processes affected by α-syn been conserved through a billion years of evolution, so have the specific protein targets on which the compounds act with only modest differences in structure-activity relationships. These studies add weight to the hypothesis that PD is a disorder of basic cellular dysfunction that certain neurons are particularly sensitive to. Our unbiased approach successfully identified individual small molecules capable of tackling multiple aspects of disease pathophysiology. These

highlight the power of using a simple model organism to elucidate complex biological processes and suggest new therapeutic strategies to treat human diseases.

Materials and Methods

Yeast Strains

Yeast strains used were in the w303 pump-deleted background (MATα can1-100, his3-11,15, leu2-3,112, trp1-1, ura3-1, ade2-1, pdr1::kanMX, pdr3::kanMX). The vector control strain contained empty vector at the trp and ura loci (pRS304Gal, pRS306GAL). The NoTox α-syn strain contained α-syn fused to green fluorescent protein (α-syn-GFP) inserted at the trp locus and empty vector at the ura locus (pRS304Gal-α-syn-GFP, pRS306GAL). The HiTox α-syn strain contained α-syn-GFP inserted at the trp and ura loci (pRS304GAL-α-syn-GFP, pRS306GAL-α-syn-GFP).

High throughput chemical screen

The high throughput screen was carried out at the Institute of Chemistry and Cell Biology and Harvard Medical School. Over 115,000 compounds from various collections including commercial libraries, natural products, NCI collections were screened in a 384-well format. HiTox yeast cells were induced in galactose media (starting OD_{600} of 0.001) and dispensed into individual wells (300 nl final) containing the test compound (17 μg/ml final in DMSO). Individual plates were incubated at 30°C for 2 days. Each compound was tested in duplicate. Each plate contained two sets of controls: cells grown in glucose media (to suppress α-syn expression), and induced α-syn cells grown in the absence of any test compound. Individual compounds were assessed for their ability to suppress α-syn toxicity by a readout in optical density (increased signal at OD_{600}) and by fluorescence microscopy (loss of aggregation).

Bioscreen

Growth curves were monitored using Bioscreen (www.bioscreen.fi). Yeast strains were pre-grown in 2% raffinose medium and induced in 2% galactose medium with starting OD_{600} of 0.1. 300 μl of induced cells were dispensed to individual wells, in presence of either the compound or vehicle control (1% DMSO final). Each growth

condition was analyzed in triplicate wells per run. Cells were grown at 30°C, with plates shaken every 30 seconds to ensure proper aeration and OD_{600} measurements taken every half hour over a two-day period. The resulting data (OD_{600} versus time) were plotted using Kaleidagraph.

Microscopy

Imaging of live yeast cells to monitor either α-syn localization with GFP was carried out as previously described (Outeiro and Lindquist, 2003).

Flow cytometry

Yeast cells were subjected to flow cytometry for measurements of reactive oxygen species (ROS) production as well as cell viability. Briefly, 500 µl of cells were treated with CM-H_2DCFDA (Invitrogen) and incubated with gentle shaking (750 rpm) at 30°C for 20' using an Eppendorf Thermomixer. These cells were briefly sonicated (to prevent clumping) before transferring into a 96 well plate and examined using an EasyCyte Flow Cytometer (Guava Technologies) and analyzed with Flowjo (Treestar). To assay for viability, 500 µl cells were briefly sonicated and treated with 10 µl of 1 mg/ml propidium iodide before proceeding with flow cytometry.

CPY pulse-chase labeling experiments

Yeast cells were grown overnight in 2% raffinose and induced in 2% galactose medium. Concurrent with the galactose induction was the addition of compound (1 µM in 1% DMSO final) or DMSO (1% final) and cells were grown at 30°C for 4.5 and 7 hours, followed by radiolabeling and immunoprecipitation as previously described (Cooper et al., 2006).

Subcellular fractionation

NoTox and HiTox αSyn-expressing strains were cultured to log phase growth in 2% raffinose-containing media prior to induction with 2% galactose for 4 hours. Cells were harvested and mitochondria isolated according to (Meisinger et al., 2006). Protein from total, crude mitochondria, and isolated mitochondria was normalized and 10 ug

protein resolved by SDS-PAGE. Western blotting with antibodies against alkaline phosphatase, *PDI1*, *PGK1*, Porin, and αSyn-GFP was used to analyze enrichment of mitochondria.

C. elegans experiments

All procedures were carried out at 25°C. Gravid P_{dat-1}::GFP + P_{dat-1}::α-synuclein adults [strain UA44 (*baIn11*)] were synchronized and embryos were obtained as previously described (Cao et al., 2005). The embryos were left in M9 buffer (22 mM KH_2PO_4, 22 mM Na_2HPO_4, 85 mM NaCl, 1 mM $MgSO_4$) in glass conical tubes with appropriate concentrations of compounds or vehicle control (time 0), and incubated at 25ºC for 24 hours to obtain relatively synchronized L1 population, followed by three M9 buffer washes. The synchronized L1 worms were then spread onto regular nematode growth media (NGM) plates seeded with 100 µl of concentrated OP_{50} *E. coli*. At 72 hours post-hatching, one hundred and twenty worms were transferred to a fresh plate containing 0.4 mg/ml 5-Fluoro-2'-deoxyuridine (FUDR) to inhibit progeny growth. The worms were analyzed at 172 hours post-hatching. Each experiment was done in triplicate and the average was calculated. The analyses of neurodegeneration were carried out according to the criteria previously described(Cao et al., 2005). For each analysis, 55-120 worms were analyzed. For worms treated at 2-day adult stages, embryos were incubated in M9 buffer after the synchronization. Two-day adult worms (94 hours post-hatching) were incubated with compound or vehicle control solutions for 8 hours and analyzed at 172 hours post-hatching.

Lentiviral transduction of α-syn-A53T

E17 rat primary mesencephalic cultures were prepared as described previously (Cooper et al., 2006). The cells were plated on coverslips at a density of 1300 cells per mm2. Four days after plating, the cells were treated with cytosine arabinofuranoside (20 µM) for 48 hours to restrict the growth of glial cells. Cultures were then incubated in fresh media for an additional 24 hours. The cells were transduced with α-syn-A53T lentivirus (MOI = 5) as described previously (Cooper et al., 2006) and incubated with the compound (applied at a sublethal dosage; data not shown) or vehicle control (DMSO). After a 72-h transduction

period, the cells were treated with fresh media for an additional 24 h prior to immunocytochemical analysis. Compounds (1)-(6), riboflavin and melatonin were applied concurrently with lentiviral transduction.

Rotenone treatment of primary mesencephalic cultures

E17 rat primary mesencephalic cultures were prepared as described above. In experiments aimed at determining the effects of the compounds on rotenone-induced toxicity, cultures were treated with rotenone (final concentration, 100 nM) and the compound or the vehicle control (DMSO) for 24-48 h prior to immunocytochemical analysis. In experiments aimed at determining the effects of Rab1 on rotenone toxicity, primary midbrain cultures were transduced with lentivirus encoding Rab1 (MOI 2). After 72 h, the cells were treated with fresh media containing rotenone (100 nM) for 24 h. Control cells were incubated in the absence of virus and then treated with fresh media supplemented with vehicle (DMSO).

Dopaminergic neuron viability assay

Immunocytochemistry was carried out as previously described (Cooper et al., 2006), using anti-MAP2 monoclonal IgG (1:500) and an anti-TH polyclonal antibody (1:500), and goat anti-rabbit IgG conjugated to AlexaFluor 488 (1:1000) and goat anti-mouse IgG conjugated to AlexaFluor 594 (1:1000). MAP2- and TH-immunoreactive primary neurons were counted in at least 10 randomly chosen observation fields for each treatment using a Nikon TE2000-U inverted fluorescence microscope with a 20x objective. The investigator responsible for counting cells was blind to the identity of the microscope slides. The data were expressed as the ratio of TH-positive neurons to MAP2-positive neurons. Each experiment was repeated at least 3 times (except for Rab1, where N = 2) using embryonic cultures isolated from independent pregnant rats. Statistical analyses were carried out using the program GraphPad Prism, Version 4.0 (http://www.graphpad.com/prism/Prism.htm).

Microarray analysis

Microarray experiments were carried out using Yeast Expression arrays from Whitehead Institute Center for Microarray Technology (WICMT). A starter culture of each sample (~ 5 ml) was grown from a single colony taken from a freshly streaked plate.

To ensure synchronous induction, an aliquot of the starter culture was inoculated into fresh media and grown overnight to early stationary phase (OD 1.0). Yeast cells were induced to a starting O.D. of 0.3 in galactose media in presence or absence of the compound (1 μM final), and harvested at 0, 2, 4, and 6 hours post-induction (50 ml aliquot per timepoint). Three biological triplicates, harvested on different days, were used for each array comparison. Total RNA was obtained using hot phenol-chloroform extraction (Schmitt et al., 1990), checked for purity by gel electrophoresis and BioAnalyzer, and labeled according to standard protocol.

Yeast Expression arrays were scanned and array data were extracted using GenePix. Data were analyzed using the limma package from Bioconductor. Spots were background corrected using a normal and exponential convolutional model, and an offset of 50 was added to reduce low-intensity noise. Expression log-ratios were normalized by print tip using loess. Differential expression was assayed at each timepoint using a moderated t-test, correcting for false discovery rate, for three pairwise comparisons between 1x α-syn, HiTox, and vector. The microarray analysis data has been deposited at the National Center for Biotechnology Information Gene Expression Omnibus (repository #GSE11633).

Thin-section EM

Thin-section EM was carried out as previously described (Gitler et al., 2008).

Acknowledgements

S.L. acknowledges support from the MGH/MIT Morris Udall Center of Excellence in Parkinson Disease Research (NS038372), the Michael J. Fox Foundation, and the Howard Hughes Medical Institute. C. elegans studies in the Caldwell laboratory were supported in part by grants from the Michael J. Fox Foundation and Howard Hughes Medical Institute. Primary midbrain culture studies in the Rochet lab were supported by grants from the National Institutes of Health (NS049221) and American Parkinson's Disease Association.

Competing interests statement

S.L. is a founder of, a former member of the Board of Directors, and has received consulting fees from FoldRx Pharmaceuticals, a company that investigates drugs to treat protein folding diseases. A.A.C. and S.L. are inventors on patents and patent applications that have been licensed to FoldRx. S.L. is also a member of the Board of Directors of Johnson & Johnson. A.A.C. and J.-C. R. have received consulting fees from FoldRx Pharmaceuticals and J.-C.R. has received payment from FoldRx for testing drugs in his laboratory.

Author contributions

L.J.S., T.F.O., P.K.A., J.A.K., and D.T. designed and performed experiments using the yeast model. L.J.S., T.F.O., P.K.A., J.A.K., D.T., and S.L. analyzed data from the yeast model. L.J.S., E.Y.L., G.W.B., E.F., and S.L. analyzed the microarray data. K.J.H. and A.A.C. designed, performed and analyzed the CPY assay. J.M.M. performed and analyzed the electron microscopy. K.E.S., F.L. and J.C.R. designed, performed and analyzed experiments involving the rat midbrain cultures. S.C., S.H., K.A.C, and G.A.C designed, performed and analyzed experiments using the *C. elegans* model. L.J.S., P.K.A. and S.L. wrote the paper.

References

Abeliovich, A., Schmitz, Y., Farinas, I., Choi-Lundberg, D., Ho, W. H., Castillo, P. E., Shinsky, N., Verdugo, J. M., Armanini, M., Ryan, A. et al. (2000). Mice lacking alpha-synuclein display functional deficits in the nigrostriatal dopamine system. *Neuron* **25**, 239-252.

Abou-Sleiman, P. M., Muqit, M. M. and Wood, N. W. (2006). Expanding insights of mitochondrial dysfunction in Parkinson's disease. *Nat Rev Neurosci* **7**, 207-219.

Attfield, P. V. (1997). Stress tolerance: the key to effective strains of industrial baker's yeast. *Nature biotechnology* **15**, 1351-1357.

Ayala, A., Venero, J. L., Cano, J. and Machado, A. (2007). Mitochondrial toxins and neurodegenerative diseases. *Front Biosci* **12**, 986-1007.

Barrell, D., Dimmer, E., Huntley, R. P., Binns, D., O'Donovan, C. and Apweiler, R. (2009). The GOA database in 2009--an integrated Gene Ontology Annotation resource. *Nucleic acids research* **37**, D396-403.

Betarbet, R., Sherer, T. B., MacKenzie, G., Garcia-Osuna, M., Panov, A. V. and Greenamyre, J. T. (2000). Chronic systemic pesticide exposure reproduces features of Parkinson's disease. *Nature neuroscience* **3**, 1301-1306.

Braak, H., Del Tredici, K., Rub, U., de Vos, R. A., Jansen Steur, E. N. and Braak, E. (2003). Staging of brain pathology related to sporadic Parkinson's disease. *Neurobiology of aging* **24**, 197-211.

Cabin, D. E., Shimazu, K., Murphy, D., Cole, N. B., Gottschalk, W., McIlwain, K. L., Orrison, B., Chen, A., Ellis, C. E., Paylor, R. et al. (2002). Synaptic vesicle depletion correlates with attenuated synaptic responses to prolonged repetitive stimulation in mice lacking alpha-synuclein. *J Neurosci* **22**, 8797-8807.

Cao, S., Gelwix, C. C., Caldwell, K. A. and Caldwell, G. A. (2005). Torsin-mediated protection from cellular stress in the dopaminergic neurons of Caenorhabditis elegans. *J Neurosci* **25**, 3801-3812.

Chandra, S., Fornai, F., Kwon, H. B., Yazdani, U., Atasoy, D., Liu, X., Hammer, R. E., Battaglia, G., German, D. C., Castillo, P. E. et al. (2004). Double-knockout mice for alpha- and beta-synucleins: effect on synaptic functions. *Proceedings of the National Academy of Sciences of the United States of America* **101**, 14966-14971.

Chen, Q., Thorpe, J. and Keller, J. N. (2005). Alpha-synuclein alters proteasome function, protein synthesis, and stationary phase viability. *The Journal of biological chemistry* **280**, 30009-30017.

Cole, N. B., Dieuliis, D., Leo, P., Mitchell, D. C. and Nussbaum, R. L. (2008). Mitochondrial translocation of alpha-synuclein is promoted by intracellular acidification. *Exp Cell Res*.

Cole, N. B., Murphy, D. D., Grider, T., Rueter, S., Brasaemle, D. and Nussbaum, R. L. (2002). Lipid droplet binding and oligomerization properties of the Parkinson's disease protein alpha-synuclein. *The Journal of biological chemistry* **277**, 6344-6352.

Cooper, A. A., Gitler, A. D., Cashikar, A., Haynes, C. M., Hill, K. J., Bhullar, B., Liu, K., Xu, K., Strathearn, K. E., Liu, F. et al. (2006). Alpha-synuclein blocks ER-Golgi traffic and Rab1 rescues neuron loss in Parkinson's models. *Science (New York, N.Y* **313**, 324-328.

Dauer, W., Kholodilov, N., Vila, M., Trillat, A. C., Goodchild, R., Larsen, K. E., Staal, R., Tieu, K., Schmitz, Y., Yuan, C. A. et al. (2002). Resistance of alpha -synuclein null mice to the parkinsonian neurotoxin MPTP. *Proceedings of the National Academy of Sciences of the United States of America* **99**, 14524-14529.

Daum, G. and Vance, J. E. (1997). Import of lipids into mitochondria. *Prog Lipid Res* **36**, 103-130.

Davis, G. C., Williams, A. C., Markey, S. P., Ebert, M. H., Caine, E. D., Reichert, C. M. and Kopin, I. J. (1979). Chronic Parkinsonism secondary to intravenous injection of meperidine analogues. *Psychiatry research* **1**, 249-254.

de Brito, O. M. and Scorrano, L. (2008). Mitofusin 2 tethers endoplasmic reticulum to mitochondria. *Nature* **456**, 605-610.

De Winde, J. H. and Grivell, L. A. (1995). Regulation of mitochondrial biogenesis in Saccharomyces cerevisiae. Intricate interplay between general and specific transcription factors in the promoter of the QCR8 gene. *European journal of biochemistry / FEBS* **233**, 200-208.

Devi, L., Raghavendran, V., Prabhu, B. M., Avadhani, N. G. and Anandatheerthavarada, H. K. (2008). Mitochondrial import and accumulation of alpha-synuclein impair complex I in human dopaminergic neuronal cultures and Parkinson disease brain. *The Journal of biological chemistry* **283**, 9089-9100.

Drolet, R. E., Behrouz, B., Lookingland, K. J. and Goudreau, J. L. (2004). Mice lacking alpha-synuclein have an attenuated loss of striatal dopamine following prolonged chronic MPTP administration. *Neurotoxicology* **25**, 761-769.

Duennwald, M. L., Jagadish, S., Muchowski, P. J. and Lindquist, S. (2006). Flanking sequences profoundly alter polyglutamine toxicity in yeast. *Proceedings of the National Academy of Sciences of the United States of America* **103**, 11045-11050.

Ellis, C. E., Murphy, E. J., Mitchell, D. C., Golovko, M. Y., Scaglia, F., Barcelo-Coblijn, G. C. and Nussbaum, R. L. (2005). Mitochondrial lipid abnormality and electron transport chain impairment in mice lacking alpha-synuclein. *Mol Cell Biol* **25**, 10190-10201.

Farrer, M., Maraganore, D. M., Lockhart, P., Singleton, A., Lesnick, T. G., de Andrade, M., West, A., de Silva, R., Hardy, J. and Hernandez, D. (2001). alpha-Synuclein gene haplotypes are associated with Parkinson's disease. *Human molecular genetics* **10**, 1847-1851.

Fleming, J., Outeiro, T. F., Slack, M., Lindquist, S. L. and Bulawa, C. E. (2008). Detection of compounds that rescue rab1-synuclein toxicity. *Methods in enzymology* **439**, 339-351.

Foley, P. and Riederer, P. (2000). Influence of neurotoxins and oxidative stress on the onset and progression of Parkinson's disease. *Journal of neurology* **247 Suppl 2**, II82-94.

Gai, W. P., Yuan, H. X., Li, X. Q., Power, J. T., Blumbergs, P. C. and Jensen, P. H. (2000). In situ and in vitro study of colocalization and segregation of alpha-synuclein, ubiquitin, and lipids in Lewy bodies. *Experimental neurology* **166**, 324-333.

Gasch, A. P., Spellman, P. T., Kao, C. M., Carmel-Harel, O., Eisen, M. B., Storz, G., Botstein, D. and Brown, P. O. (2000). Genomic expression programs in the response of yeast cells to environmental changes. *Molecular biology of the cell* **11**, 4241-4257.

Gitler, A. D., Chesi, A., Geddie, M. L., Strathearn, K. E., Hamamichi, S., Hill, K. J., Caldwell, K. A., Caldwell, G. A., Cooper, A. A., Rochet, J. C. et al. (2009). alpha-Synuclein is part of a diverse and highly conserved interaction network that includes PARK9 and manganese toxicity. *Nat Genet*.

Gitler, A. D., Bevis, B. J., Shorter, J., Strathearn, K. E., Hamamichi, S., Su, L. J., Caldwell, K. A., Caldwell, G. A., Rochet, J. C., McCaffery, J. M. et al. (2008). The Parkinson's disease protein alpha-synuclein disrupts cellular Rab homeostasis. *Proceedings of the National Academy of Sciences of the United States of America* **105**, 145-150.

Hoepken, H. H., Gispert, S., Azizov, M., Klinkenberg, M., Ricciardi, F., Kurz, A., Morales-Gordo, B., Bonin, M., Riess, O., Gasser, T. et al. (2008). Parkinson patient fibroblasts show increased alpha-synuclein expression. *Experimental neurology* **212**, 307-313.

Hong, E. L., Balakrishnan, R., Dong, Q., Christie, K. R., Park, J., Binkley, G., Costanzo, M. C., Dwight, S. S., Engel, S. R., Fisk, D. G. et al. (2008). Gene Ontology annotations at SGD: new data sources and annotation methods. *Nucleic acids research* **36**, D577-581.

Ibanez, P., Lesage, S., Janin, S., Lohmann, E., Durif, F., Destee, A., Bonnet, A. M., Brefel-Courbon, C., Heath, S., Zelenika, D. et al. (2009). Alpha-synuclein gene rearrangements in dominantly inherited parkinsonism: frequency, phenotype, and mechanisms. *Archives of neurology* **66**, 102-108.

Jo, E., McLaurin, J., Yip, C. M., St George-Hyslop, P. and Fraser, P. E. (2000). alpha-Synuclein membrane interactions and lipid specificity. *The Journal of biological chemistry* **275**, 34328-34334.

Kandel, E., Schwartz, J., Jessel, T. (2000). Principles of Neural Science. New York: McGraw-Hill Company.

Kay, D. M., Factor, S. A., Samii, A., Higgins, D. S., Griffith, A., Roberts, J. W., Leis, B. C., Nutt, J. G., Montimurro, J. S., Keefe, R. G. et al. (2008). Genetic association between alpha-synuclein and idiopathic Parkinson's disease. *Am J Med Genet B Neuropsychiatr Genet* **147B**, 1222-1230.

Klivenyi, P., Siwek, D., Gardian, G., Yang, L., Starkov, A., Cleren, C., Ferrante, R. J., Kowall, N. W., Abeliovich, A. and Beal, M. F. (2006). Mice lacking alpha-synuclein are resistant to mitochondrial toxins. *Neurobiol Dis* **21**, 541-548.

Kornmann, B., Currie, E., Collins, S. R., Schuldiner, M., Nunnari, J., Weissman, J. S. and Walter, P. (2009). An ER-Mitochondria Tethering Complex Revealed by a Synthetic Biology Screen. *Science (New York, N.Y.*

Kritzer, J. A., Hamamichi, S., McCaffery, J. M., Santagata, S., Naumann, T. A., Caldwell, K. A., Caldwell, G. A. and Lindquist, S. (2009). Rapid selection of cyclic peptides that reduce alpha-synuclein toxicity in yeast and animal models. *Nature chemical biology*.

Kruger, R., Kuhn, W., Muller, T., Woitalla, D., Graeber, M., Kosel, S., Przuntek, H., Epplen, J. T., Schols, L. and Riess, O. (1998). Ala30Pro mutation in the gene encoding alpha-synuclein in Parkinson's disease. *Nat Genet* **18**, 106-108.

Langston, J. W., Ballard, P., Tetrud, J. W. and Irwin, I. (1983). Chronic Parkinsonism in humans due to a product of meperidine-analog synthesis. *Science (New York, N.Y* **219**, 979-980.

Liu, F., Nguyen, J. L., Hulleman, J. D., Li, L. and Rochet, J. C. (2008a). Mechanisms of DJ-1 neuroprotection in a cellular model of Parkinson's disease. *Journal of neurochemistry*.

Liu, F., Hindupur, J., Nguyen, J. L., Ruf, K. J., Zhu, J., Schieler, J. L., Bonham, C. C., Wood, K. V., Davisson, V. J. and Rochet, J. C. (2008b). Methionine sulfoxide reductase A protects dopaminergic cells from Parkinson's disease-related insults. *Free radical biology & medicine* **45**, 242-255.

Liu, Z., Sekito, T., Spirek, M., Thornton, J. and Butow, R. A. (2003). Retrograde signaling is regulated by the dynamic interaction between Rtg2p and Mks1p. *Molecular cell* **12**, 401-411.

Louvion, J. F., Havaux-Copf, B. and Picard, D. (1993). Fusion of GAL4-VP16 to a steroid-binding domain provides a tool for gratuitous induction of galactose-responsive genes in yeast. *Gene* **131**, 129-134.

Mandemakers, W., Morais, V. A. and De Strooper, B. (2007). A cell biological perspective on mitochondrial dysfunction in Parkinson disease and other neurodegenerative diseases. *Journal of cell science* **120**, 1707-1716.

Martin, L. J., Pan, Y., Price, A. C., Sterling, W., Copeland, N. G., Jenkins, N. A., Price, D. L. and Lee, M. K. (2006). Parkinson's disease alpha-synuclein transgenic mice develop neuronal mitochondrial degeneration and cell death. *J Neurosci* **26**, 41-50.

Meisinger, C., Pfanner, N. and Truscott, K. N. (2006). Isolation of yeast mitochondria. *Methods Mol Biol* **313**, 33-39.

Mosharov, E. V., Larsen, K. E., Kanter, E., Phillips, K. A., Wilson, K., Schmitz, Y., Krantz, D. E., Kobayashi, K., Edwards, R. H. and Sulzer, D. (2009). Interplay between cytosolic dopamine, calcium, and alpha-synuclein causes selective death of substantia nigra neurons. *Neuron* **62**, 218-229.

Murphy, D. D., Rueter, S. M., Trojanowski, J. Q. and Lee, V. M. (2000). Synucleins are developmentally expressed, and alpha-synuclein regulates the size of the presynaptic vesicular pool in primary hippocampal neurons. *J Neurosci* **20**, 3214-3220.

Norris, E. H., Giasson, B. I., Ischiropoulos, H. and Lee, V. M. (2003). Effects of oxidative and nitrative challenges on alpha-synuclein fibrillogenesis involve distinct mechanisms of protein modifications. *The Journal of Biological Chemistry* 278, 27230-27240.

Norris, E. H., Uryu, K., Leight, S., Giasson, B. I., Trojanowski, J. Q. and Lee, V. M. (2007). Pesticide exposure exacerbates alpha-synucleinopathy in an A53T transgenic mouse model. *The American journal of pathology* **170**, 658-666.

Outeiro, T. F. and Lindquist, S. (2003). Yeast cells provide insight into alpha-synuclein biology and pathobiology. *Science (New York, N.Y* **302**, 1772-1775.

Parihar, M. S., Parihar, A., Fujita, M., Hashimoto, M. and Ghafourifar, P. (2008). Mitochondrial association of alpha-synuclein causes oxidative stress. *Cell Mol Life Sci* **65**, 1272-1284.

Polymeropoulos, M. H., Lavedan, C., Leroy, E., Ide, S. E., Dehejia, A., Dutra, A., Pike, B., Root, H., Rubenstein, J., Boyer, R. et al. (1997). Mutation in the alpha-synuclein gene identified in families with Parkinson's disease. *Science (New York, N.Y* **276**, 2045-2047.

Rideout, H. J., Dietrich, P., Wang, Q., Dauer, W. T. and Stefanis, L. (2004). alpha-synuclein is required for the fibrillar nature of ubiquitinated inclusions induced by proteasomal inhibition in primary neurons. *The Journal of biological chemistry* **279**, 46915-46920.

Schmitt, M. E., Brown, T. A. and Trumpower, B. L. (1990). A rapid and simple method for preparation of RNA from Saccharomyces cerevisiae. *Nucleic acids research* **18**, 3091-3092.

Scholz, S. W., Houlden, H., Schulte, C., Sharma, M., Li, A., Berg, D., Melchers, A., Paudel, R., Gibbs, J. R., Simon-Sanchez, J. et al. (2009). SNCA variants are associated with increased risk for multiple system atrophy. *Annals of neurology* **65**, 610-614.

Sharma, N., Brandis, K. A., Herrera, S. K., Johnson, B. E., Vaidya, T., Shrestha, R. and Debburman, S. K. (2006). alpha-Synuclein budding yeast model: toxicity enhanced by impaired proteasome and oxidative stress. *J Mol Neurosci* **28**, 161-178.

Sherer, T. B., Kim, J. H., Betarbet, R. and Greenamyre, J. T. (2003). Subcutaneous rotenone exposure causes highly selective dopaminergic degeneration and alpha-synuclein aggregation. *Experimental neurology* **179**, 9-16.

Singleton, A. B., Farrer, M., Johnson, J., Singleton, A., Hague, S., Kachergus, J., Hulihan, M., Peuralinna, T., Dutra, A., Nussbaum, R. et al. (2003). alpha-Synuclein locus triplication causes Parkinson's disease. *Science (New York, N.Y* **302**, 841.

Smith, W. W., Jiang, H., Pei, Z., Tanaka, Y., Morita, H., Sawa, A., Dawson, V. L., Dawson, T. M. and Ross, C. A. (2005). Endoplasmic reticulum stress and mitochondrial cell death pathways mediate A53T mutant alpha-synuclein-induced toxicity. *Human molecular genetics* **14**, 3801-3811.

Song, D. D., Shults, C. W., Sisk, A., Rockenstein, E. and Masliah, E. (2004). Enhanced substantia nigra mitochondrial pathology in human alpha-synuclein transgenic mice after treatment with MPTP. *Experimental neurology* **186**, 158-172.

Soper, J. H., Roy, S., Stieber, A., Lee, E., Wilson, R. B., Trojanowski, J. Q., Burd, C. G. and Lee, V. M. (2008). Alpha-synuclein-induced aggregation of cytoplasmic vesicles in Saccharomyces cerevisiae. *Molecular biology of the cell* **19**, 1093-1103.

Spillantini, M. G., Schmidt, M. L., Lee, V. M., Trojanowski, J. Q., Jakes, R. and Goedert, M. (1997). Alpha-synuclein in Lewy bodies. *Nature* **388**, 839-840.

Spillantini, M. G., Crowther, R. A., Jakes, R., Cairns, N. J., Lantos, P. L. and Goedert, M. (1998). Filamentous alpha-synuclein inclusions link multiple system atrophy with Parkinson's disease and dementia with Lewy bodies. *Neuroscience letters* **251**, 205-208.

Stichel, C. C., Zhu, X. R., Bader, V., Linnartz, B., Schmidt, S. and Lubbert, H. (2007). Mono- and double-mutant mouse models of Parkinson's disease display severe mitochondrial damage. *Human molecular genetics* **16**, 2377-2393.

Van Laar, V. S. and Berman, S. B. (2009). Mitochondrial dynamics in Parkinson's disease. *Experimental neurology*.

Vander Heiden, M. G., Chandel, N. S., Williamson, E. K., Schumacker, P. T. and Thompson, C. B. (1997). Bcl-xL regulates the membrane potential and volume homeostasis of mitochondria. *Cell* **91**, 627-637.

Yeger-Lotem, E., Riva, L., Su, L. J., Gitler, A. D., Cashikar, A. G., King, O. D., Auluck, P. K., Geddie, M. L., Valastyan, J. S., Karger, D. R. et al. (2009). Bridging high-throughput genetic and transcriptional data reveals cellular responses to alpha-synuclein toxicity. *Nat Genet* **41**, 316-323.

Figure Legends

Fig. 1 Transcriptional profiling of yeast expressing α-syn revealed mitochondrial stress as a key signature in α-syn toxicity. **A.** Profiles of 673 genes exhibiting differential expression in at least one experiment (compared against Vector) at 2 and 4 hours post α-syn induction (p-value<0.05; >2-fold) are shown. These genes exhibited very little changes in NoTox cells. In contrast, some of these genes were differentially expressed in HiTox cells as early as 2 hours post-induction, well before onset of toxicity (at 4 hours). In contrast to treatment with inactive compounds (**5**) and (**6**), treatment with active compounds **(1**), (**2**), and (**4**) resulted in a major reduction of transcriptional changes, indicating rescue. Differentially expressed genes were color-coded in red (upregulated) and green (downregulated). **B.** GO annotation of differentially regulated genes (>2-fold) revealed upregulation in the expression of oxidoreductase transcripts and down-regulation in the expression of mitochondrial, ribosomal, respiratory and carbohydrate transport transcripts in HiTox α-syn cells induced for 4 hours. The expression of transition metal ion binding transcripts was both up- and downregulated. Similar, more subtle changes were detects in HiTox cells after 2 hours of induction. Only slight downregulation of carbohydrate transport transcripts were detected in NoTox cells after 4 hours of induction. **C.** Treatment with compounds (**1**) or (**2**) markedly reversed the HiTox-induced transcriptional changes in the ribosomal, mitochondrial, respiratory, and oxidoreductase GO categories. Compound (**4**) showed a more modest transcriptional restoration in these categories. Compounds (**5**) and (**6**) exhibited partial reversal of the α-syn induced transcriptional changes in these GO categories, however, the magnitude of this reversal was less complete that that seen in cells treated with compounds (**1**), (**2**), or (**4**).

Fig. 2. HiTox cells exhibit mitochondrial abnormalities. **A.** Thin section EM of HiTox cells at 4 hours post-induction. NoTox cells (b) exhibited comparable features to those of cells expressing vector (a), whereas HiTox cells exhibited numerous defects, including vesicular accumulation, swollen and less electron-dense mitochondria, and hypertrophied ER (c, and inset). Legends: m = mitochondria, n = nucleus, v = vacuole. An asterisk denotes the vesicle clusters. Scale bar = 1.0 μm. **B.** Reactive oxygen species (ROS) production was measured using CM-H_2DCFDA. Vector or NoTox cells had very little or

no ROS, whereas nearly 35% of HiTox cells exhibited ROS. ROS reactivity in HiTox cells was ameliorated upon treatment with (**1**) – (**4**) (<15%), but not with (**5**) or (**6**) (>25%). Bar graph shows the mean ± s.e.m.. from at least three independent experiments, and an asterisk (*) represents a value that significantly differed from that of HiTox, with p-value less than 0.05 as determined by two-tailed Student's t-test. **C**. Subcellular fractionation shows little α-syn in the mitochondria. NoTox and HiTox strains were subjected to cellular fractionation to track compartmentalization of α-synGFP. Western blots (left) and coomassie staining (right) of three fractions are shown: total lysate (S4,000), crude mitochondrial pellet (P13,000), and gradient purified mitochondria (Mito.). Western blot analysis shows the specific enrichment for mitochondria in the gradient (Porin). P13,000 fraction contains vacuole, ER, and mitochondria while most α-synGFP remains soluble in S13,000. Only mitochondria are highly enriched by the sucrose step gradient with most α-synGFP eliminated from this fraction. Quantitative western analysis with the Licor Odyssey infrared imaging (data not shown) revealed that only 0.11% (NoTox) and 0.02% (HiTox) of α-synGFP localized to mitochondria. The absolute amount of mitochondrial α-synGFP does not change, rather the difference between NoTox and HiTox is a function of higher total α-synGFP levels in the HiTox strain.

Fig. 3 A high-throughput chemical screen identified small molecule antagonists of α-syn toxicity. **A**. Secondary screen identified 4 bioactive molecules rescuing at μM concentration, as well as 2 biologically inactive molecules, all representing the same chemical family. **B.** Growth curve of HiTox cells (black curve), which did not grow. Bioactive compound (**3**) was maximally effective at 1 μM, restoring growth of HiTox cells up to nearly 50% of that for wild-type cells (Fig. S5) at 48 hours post-induction. **C**. Growth of HiTox cells was rescued by treatment with 1 μM of the bioactive compounds ((**1**), (**2**), (**3**), (**4**)), but not by compounds (**5**) or (**6**). These differences were consistent over three different experiments but that slight differences in starting OD and room temperature/humidity prohibit averaging across experiments. **D.** Propidium iodide (PI) staining for cell viability revealed ~ 25% toxicity in HiTox cells at 6 hours after induction. Treating HiTox cells with 1 μM (**3**) restored viability (by reducing toxicity to < 10%),

whereas (**5**) had no significant effect. The bar graph shows the mean ± s.e.m... from at least three independent experiments, and an asterisk (*) represents a value that significantly differed from that of HiTox, with p-value less than 0.05 as determined by two-tailed Student's t-test.

Fig. 4 Validation of lead compounds in higher order model systems. **A-C**. *C. elegans* model w/ α-syn over-expression in dopaminergic neurons. Blinded assay identified compounds (**1**), (**2**), (**3**), (**4**) as active, and compounds (**5**) and (**6**) as inactive. (**A-B** bar graph showing number of worms with all 4 intact CEP neurons in each treatment; **A**, Embryo; **B**, adult worms; The bar graph shows the mean ± s.d. from at least three independent experiments, and an asterisk (*) represents a value that significantly differed (p-value < 0.05; two-tailed Student's t-test) from that of α-syn worms receiving only the vehicle DMSO. **C**. Photo of GFP-tagged neurons in each type of treatment. Importantly, these compounds exerted a rescue in adult worms that have been over-expressing α-syn for some time (B). **D-E.** Primary midbrain culture model, in which cells were transfected with lentivirus encoding α-syn A53T mutation. **D.** Immunofluorescence (IF) images of midbrain cultures. Transduction with A53T lentivirus led to abnormal neuronal morphology, including loss of bipolar neuronal processes and shrunken cell bodies. These effects are partially reversed in cultures treated with (**1**), but not (**5**). Red, MAP2 marker; Green, TH marker; Yellow, overlap. Scale bar, 20 μm. **E.** Blinded assay carried out in cultures transduced with α-syn-A53T lentivirus identified compounds (**1**), (**2**), (**3**), and (**6**) as suppressors. The concentrations of these compounds on the bar graph were as follows: (**1**), 0.5 μg/ml; (**2**), 1.0 μg/ml; (**3**), 0.25 μg/ml; (**4**), 0.125 μg/ml; (**5**), 0.05 μg/ml; (**6**), 1.0 μg/ml. The bar graph shows the mean ± s.e.m.. from at least four independent experiments, and an asterisk (*) represents a significant difference with respect to the value obtained for cells expressing A53T-α-syn in the absence of compound (p-value < 0.05; one-way ANOVA with Newman-Keuls post-test).

Fig. 5 The bioactive compounds restored aSyn membrane localization, ER to Golgi trafficking, and mitochondrial morphology. **A.** Microscopy studies with GFP-tagged α-

syn at 4 hours post-induction showed α-syn foci in HiTox cells. Localization of α-syn was restored to the plasma membrane upon treatment with the bioactive compounds. In contrast, bright foci were retained in cells treated with inactive compounds. **B.** CPY maturation assay. The bar graph depicts the percentage of CPY that exits ER and entered Golgi or the vacuole in various treatments. At 4.5 hours post-induction, HiTox cells exhibited severe trafficking defects, as majority of CPY was retained in the ER (~ 65%; DMSO and data not shown). This defect was suppressed by cells treated with 1 μM of the bioactive compounds [(**1**), (**2**), (**3**), and (**4**)], but not by the inactive compounds [(**5**), (**6**)]. Gel slices (left), bar graph shows the mean± s.e.m... (**right**). **C.** Treatment with 1 μM (**1**) - (**4**) (a-d), but not with (**5**) or (**6**) (e-f), restored ER as well as most of the mitochondria to normal morphology, but some vesicular accumulation persisted. Legends: m = mitochondria, n = nucleus, v = vacuole. An asterisk denotes the vesicle clusters. Scale bar = 1.0 μm.

Fig. 6 Effect of lead compounds on rotenone neurotoxicity. **A.** Immunofluorescence (IF) images of the primary midbrain cultures. Treatment with (**1**) dramatically restored the neuronal morphology of rotenone-treated neurons. Red, MAP2 marker; Green, TH marker; Yellow, overlap. Scale bar, 20 μm. **B.** Exposure to 100 nM rotenone resulted in >50% death of dopaminergic neurons, whereas compound (**1**) antagonized rotenone-induced dopaminergic cell death in a concentration-dependent manner. The bar graph shows the mean ± s.e.m... from at least three independent experiments, and asterisks (***) represent a significant difference with respect to the value obtained for cells exposed to rotenone alone (p-value < 0.001; one-way ANOVA with Dunnett's post-test).

Supplemental Figure Legends

Supplemental Fig. S1 High levels of α-syn expression (HiTox) elicit measurable levels of cell death by propidium iodide after 4 hours of induction in galactose media. No cell death is detected in cells expressing non-toxic levels of α-syn (NoTox).

Supplemental Fig. S2 The yeast inactive compound (**5**) competitively inhibits the cytoprotective activity of compound (**3**). Growth of vector (**A**) and HiTox α-syn cells (**B**)

were measured for a period of 48 hours. **A.** Treatment with compound (**3**), (**5**), or both did not alter the growth of the vector cells. **B.** Treatment with 1 μM compound (**3**) modestly increased the growth of HiTox α-syn cells. This rescue by compound (**3**) was blocked by the addition of compound (**5**) in a dose-dependant manner.

Supplemental Fig. S3 Suppression of α-syn toxicity by the active compounds is still seen using estradiol-induction of α-syn expression in galactose-free media. An estradiol-inducible transactivator was introduced to control the expression of α-syn. Cell death was measured using propidium iodide. Cell death in HiTox α-syn cells was suppressed by 1 μM compounds (**1**) – (**4**) but not by compounds (**5**) or (**6**).

Supplemental Fig. S4 Compound (**4**) does not suppress the toxicity of huntingtin-72Q in yeast cells. The growth of yeast expressing exon 1 of huntingtin with a 72 repeat glutamine expansion was measured for a period of 48 hours of induction in galactose. Treatment with up to 50 μM compound (**4**) did not alter the toxicity of huntingtin-72Q to yeast cells.

Supplemental Fig. S5 Compounds (**1**) and (**4**) do not alter the rate of α-syn fibril formation. α-Syn fibers were assembled under standard conditions in the presence of stoichiometric quantities of either compound (**1**) or (**4**) and the rate of fibril formation waas monitered by thioflavin T fluorescence at 490 nm.

Supplemental Fig. S6 Compounds (**3**), (**4**), and (**5**) protect against the toxicity of rotenone to dopaminergic neurons in rat midbrain cultures. Rat midbrain cultures were exposed to 100 nM rotenone or vehicle for 24-48 hours prior to immunocytochemical analysis. **A.** Treatment with 0.5 μg/mL compound (**4**) significantly suppressed the toxicity of rotenone. Higher concentrations of compound (**4**) (2 μg/mL) were less effective. **B.** Treatment with 0.05 μg/mL compound (**3**) or 0.25 μg/mL compound (**5**) also demonstrated neuroprotective activity, although treatment with compound (**3**) did not reach statistical significance. **C.** Overexpression of mRab1, which antagonizes α-syn toxicity, did not suppress the toxicity of rotenone to dopaminergic neurons in the rat midbrain cultures. (* p-value <0.05, ** p-

value <0.01, ***p-value <0.001, N.S. not significant; One-way ANOVA with Newman Keuls post-test.)

Supplemental Fig. S7 N-acetylcysteine (NAC) protects against oxidative stress but not α-syn toxicity. **A.** Vector control cells were exposed to H_2O_2 for 1 hour before assaying for generation of reactive oxygen species (ROS; CM-H_2DCFDA). Treatment with 1-25 mM NAC reduced the amount of ROS generated by H_2O_2 exposure. Compound (**3**) did not reduce the generation of ROS due to H_2O_2. **B.** HiTox α-syn cells were treated with vehicle, 1-25 mM NAC, or 1 μM compound (**3**) for 6 hours before assaying for cell viability using propidium iodide labeling. NAC was not protective against the toxicity of α-syn. (* p-value <0.05).

Supplemental Fig. S8 Melatonin protects against oxidative stress but not α-syn toxicity. **A.** Vector control cells were exposed to H_2O_2 for 1 hour before assaying for cell death (PI labeling). Treatment with 100 uM melatonin reduced PI labeling from 12% to 4%, the level of PI labeling also seen in cells not exposed to H_2O_2. **B.** Treatment with melatonin did not reverse the growth inhibition seen in HiTox α-syn cells over a 24 hour treatment period.

Supplemental Fig. S9 Riboflavin protects against oxidative stress but not α-syn toxicity. *Top*, Exposure to H_2O_2 yielded modest toxicity in vector cells. This toxicity was partially ameliorated upon treatment with riboflavin. *Bottom,* Riboflavin did not ameliorate α-syn toxicity in the IntTox or HiTox strains.

Supplemental Fig. S10 Treatment with neither N-acetylcysteine (NAC) nor ascorbic acid protected against the toxicity of α-syn to CEP neurons in *C. elegans*. Treatment with compound (**3**) increased the preservation of CEP neurons to 50% of animals. Treatment with NAC or ascorbic acid did not alter the preservation of CEP neurons. (* p-value < 0.05)

Supplemental Fig. S11 Treatment with neither melatonin nor riboflavin protected against the toxicity of α-syn-A53T to dopaminergic neurons in the primary rat neuronal cultures. Rat midbrain cultures were treated with 0.1% DMSO (**A**), 1 μM melatonin (**B**), or 10 μM riboflavin (**C**).

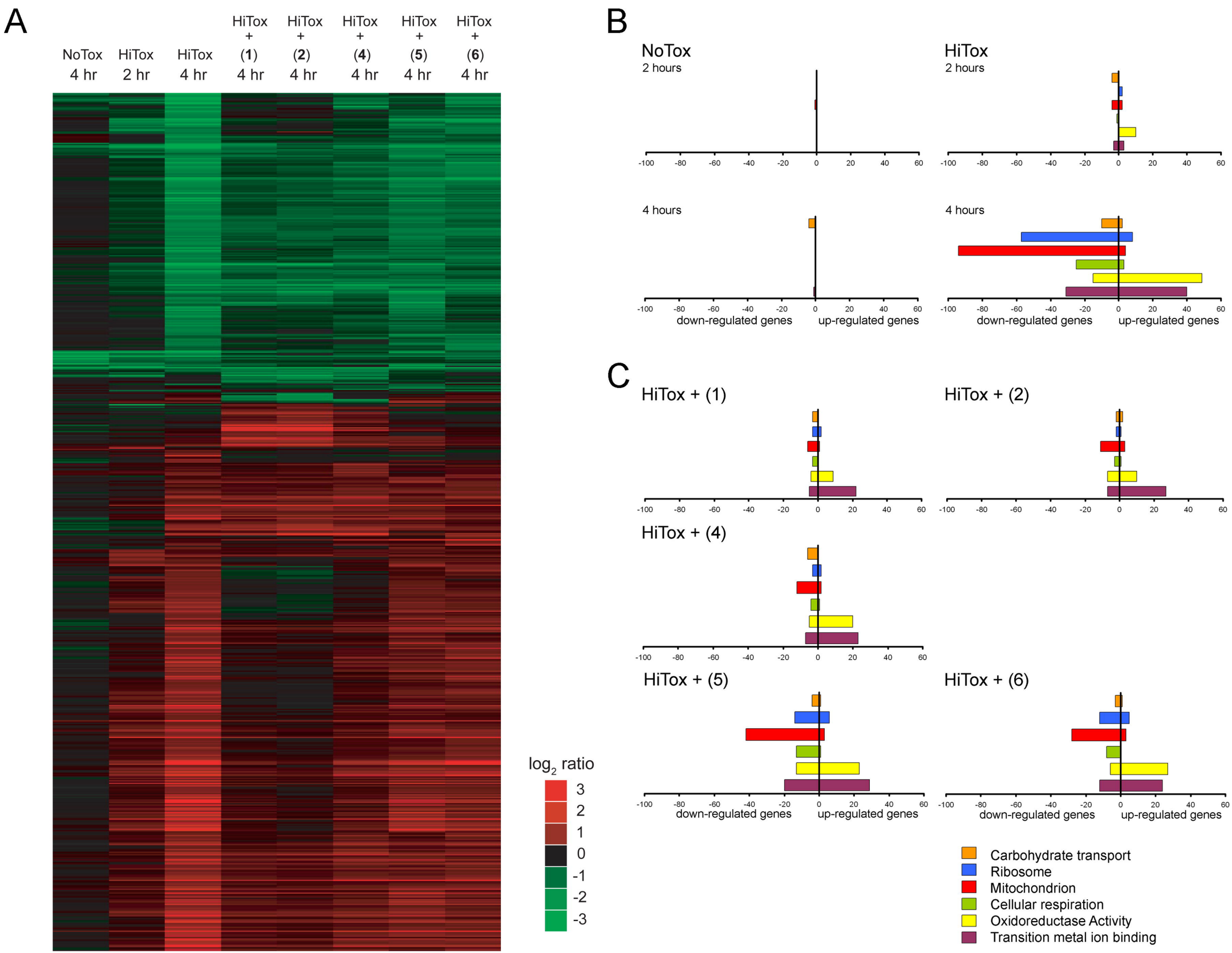
A
NoTox 4 hr
HiTox 2 hr
HiTox 4 hr
HiTox + (1) 4 hr
HiTox + (2) 4 hr
HiTox + (4) 4 hr
HiTox + (5) 4 hr
HiTox + (6) 4 hr
log2 ratio
3
2
1
0
-1
-2
-3
B
NoTox
2 hours
HiTox
2 hours
4 hours
4 hours
-100 -80 -60 -40 -20 0 20 40 60
down-regulated genes
up-regulated genes
C
HiTox + (1)
HiTox + (2)
HiTox + (4)
HiTox + (5)
HiTox + (6)
Carbohydrate transport
Ribosome
Mitochondrion
Cellular respiration
Oxidoreductase Activity
Transition metal ion binding

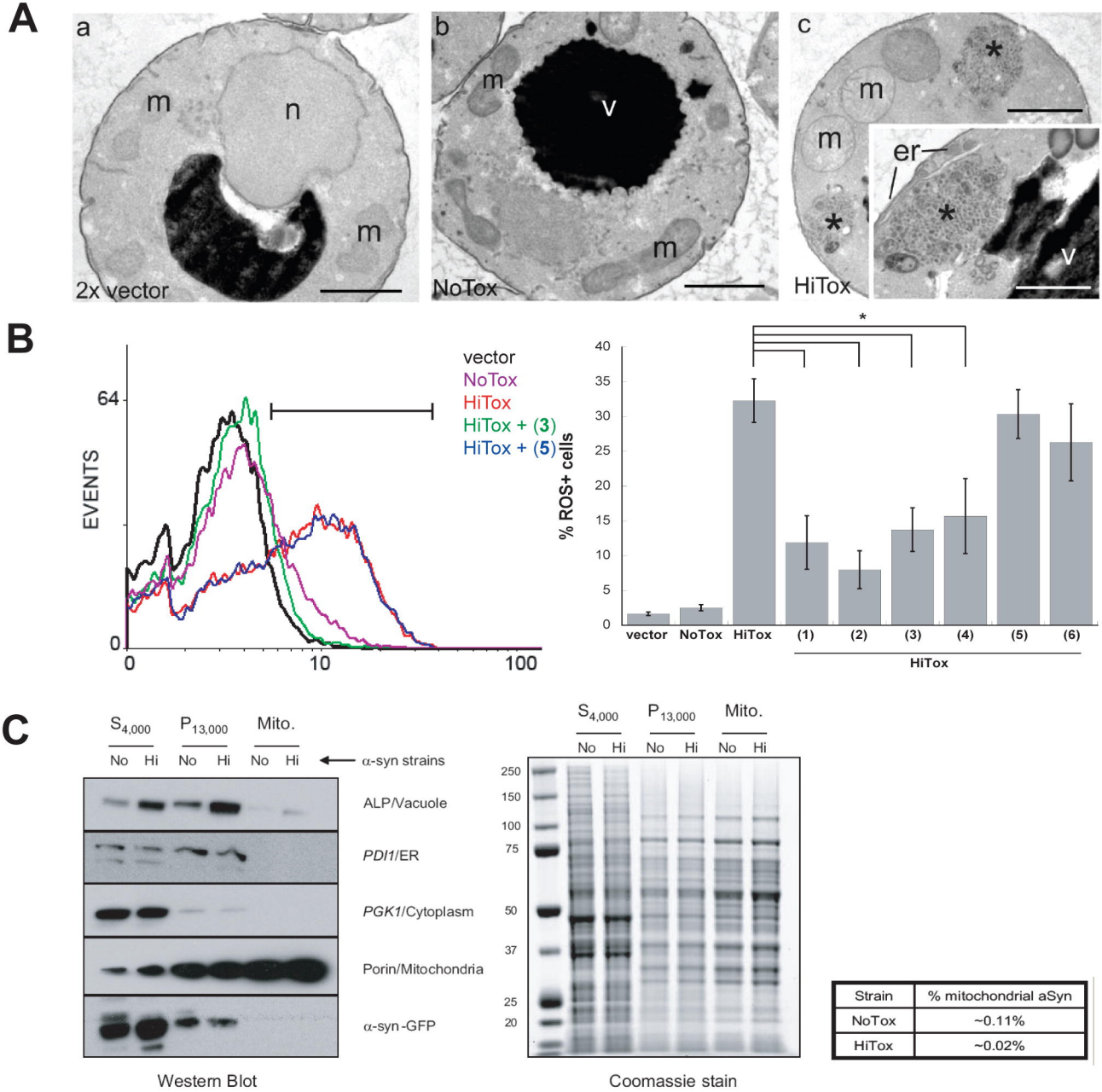
A
a
m
n
m
2x vector
b
m
v
m
NoTox
c
m
m
*
*
er
*
v
HiTox
B
vector
NoTox
HiTox
HiTox + (3)
HiTox + (5)
64
EVENTS
0
0
10
100
% ROS+ cells
40
35
30
25
20
15
10
5
0
*
vector
NoTox
HiTox
(1)
(2)
(3)
(4)
(5)
(6)
HiTox
C
S4,000
P13,000
Mito.
No Hi No Hi No Hi
α-syn strains
ALP/Vacuole
PDI1/ER
PGK1/Cytoplasm
Porin/Mitochondria
α-syn-GFP
Western Blot
S4,000
P13,000
Mito.
No Hi No Hi No Hi
250
150
100
75
50
37
25
20
Coomassie stain
Strain
% mitochondrial aSyn
NoTox
~0.11%
HiTox
~0.02%

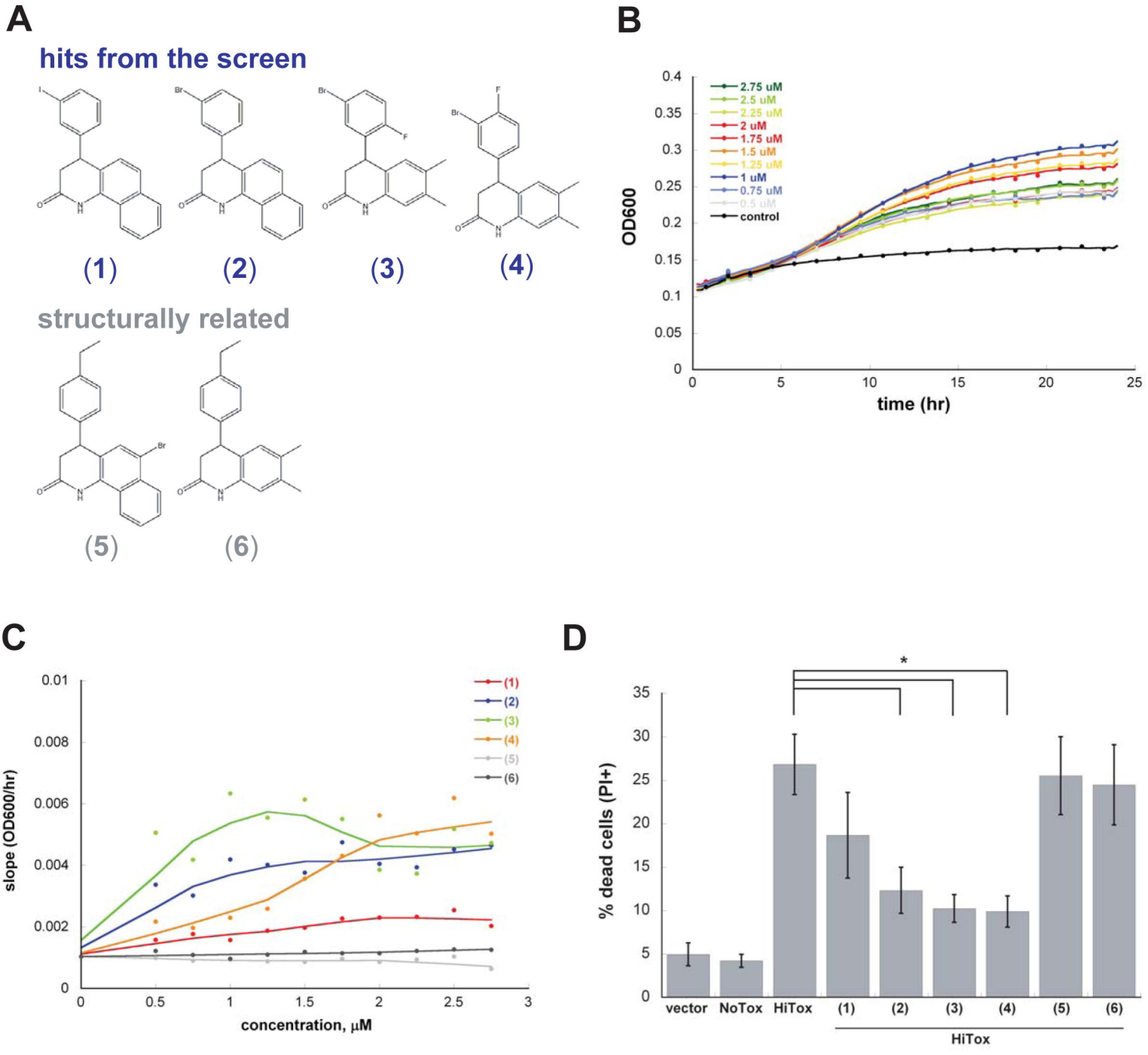
A
hits from the screen
(1)
(2)
(3)
(4)
structurally related
(5)
(6)
B
2.75 uM
2.5 uM
2.25 uM
2 uM
1.75 uM
1.5 uM
1.25 uM
1 uM
0.75 uM
0.5 uM
control
OD600
time (hr)
C
slope (OD600/hr)
concentration, μM
D
% dead cells (PI+)
vector
NoTox
HiTox
HiTox

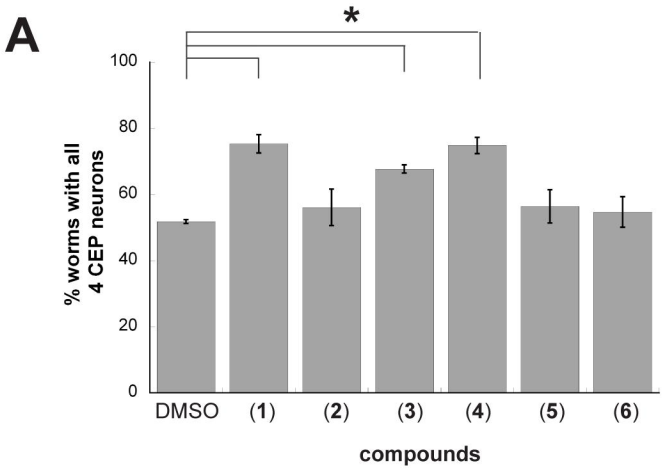
A
*
100
80
60
40
20
0
% worms with all 4 CEP neurons
DMSO
(1)
(2)
(3)
(4)
(5)
(6)
compounds

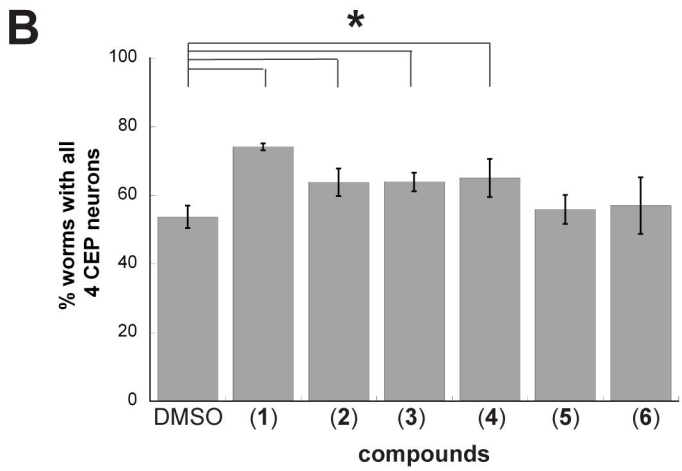
B
*
100
80
60
40
20
0
% worms with all 4 CEP neurons
DMSO
(1)
(2)
(3)
(4)
(5)
(6)
compounds

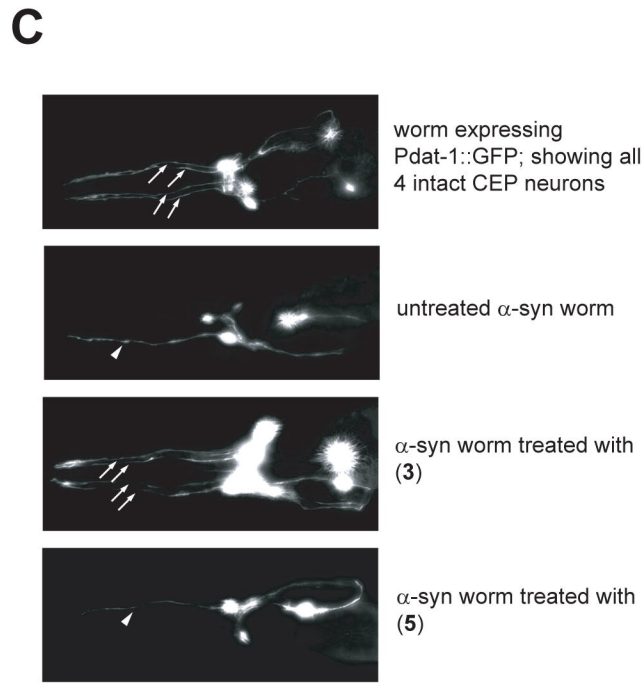
C
worm expressing Pdat-1::GFP; showing all 4 intact CEP neurons
untreated α-syn worm
α-syn worm treated with (3)
α-syn worm treated with (5)

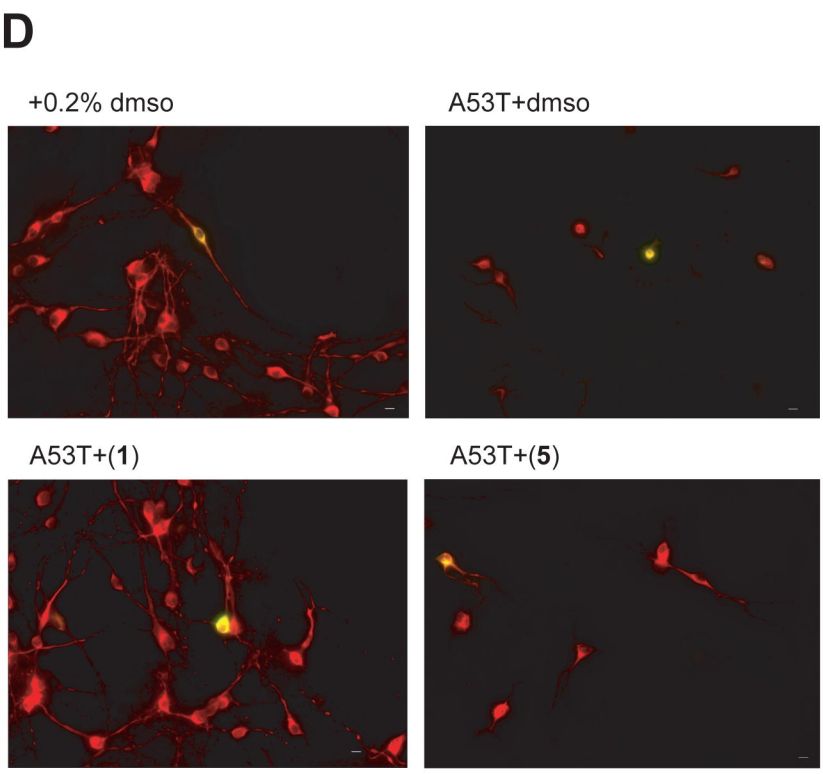
D
+0.2% dmso
A53T+dmso
A53T+(1)
A53T+(5)

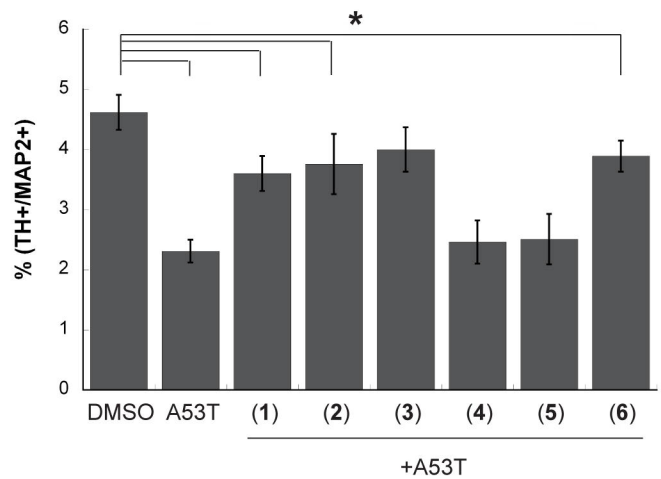
E
*
6
5
4
3
2
1
0
% (TH+/MAP2+)
DMSO
A53T
(1)
(2)
(3)
(4)
(5)
(6)
+A53T

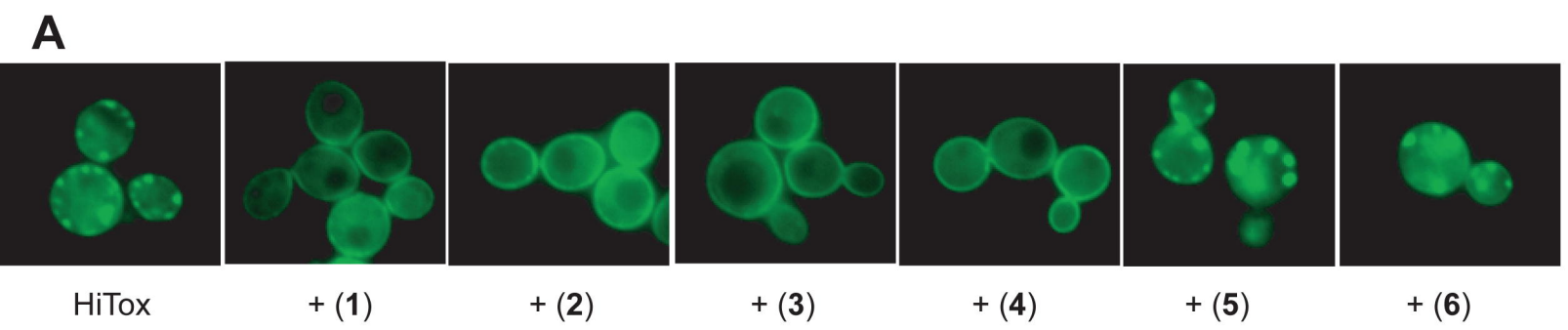
A
HiTox
+ (1)
+ (2)
+ (3)
+ (4)
+ (5)
+ (6)

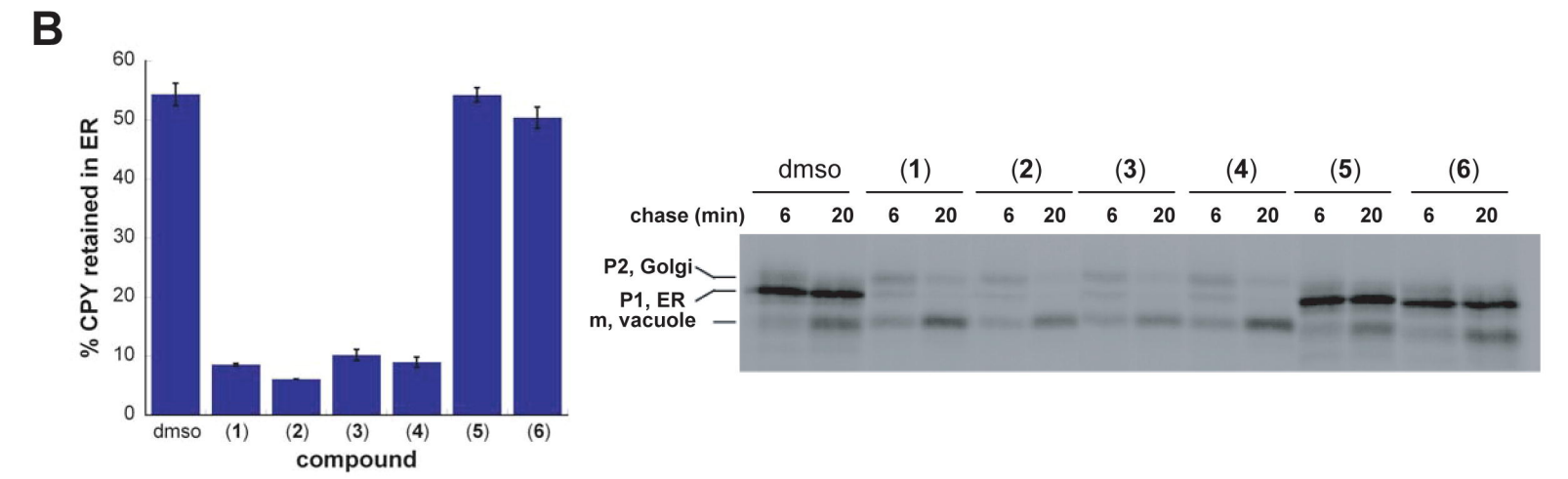
B
% CPY retained in ER
60
50
40
30
20
10
0
dmso
(1)
(2)
(3)
(4)
(5)
(6)
compound
dmso
(1)
(2)
(3)
(4)
(5)
(6)
chase (min)
6
20
P2, Golgi
P1, ER
m, vacuole

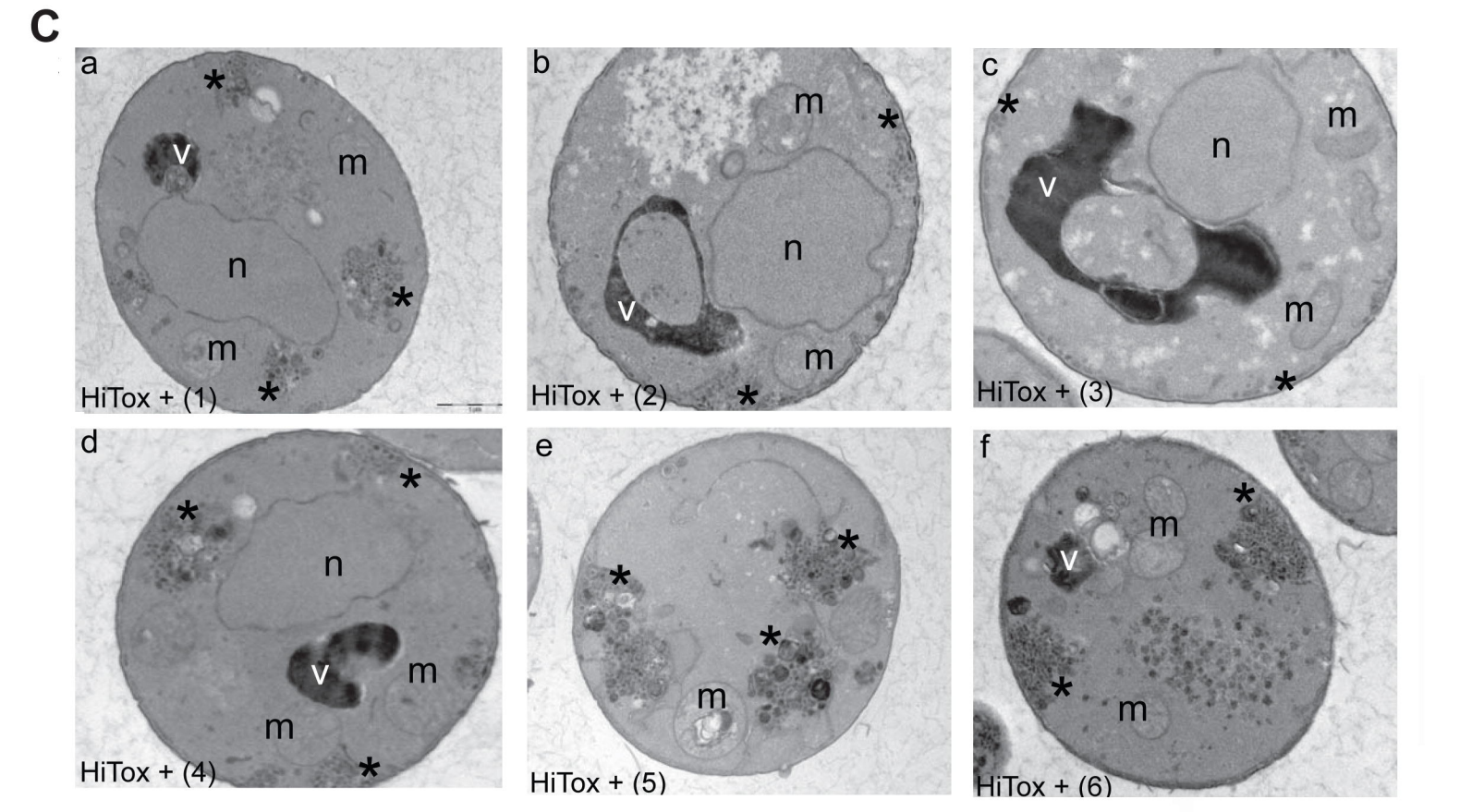
C
a
HiTox + (1)
b
HiTox + (2)
c
HiTox + (3)
d
HiTox + (4)
e
HiTox + (5)
f
HiTox + (6)
v
m
n
*

A

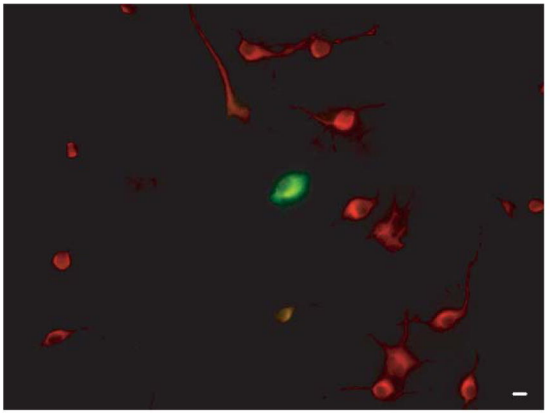
rotenone (100 nM)

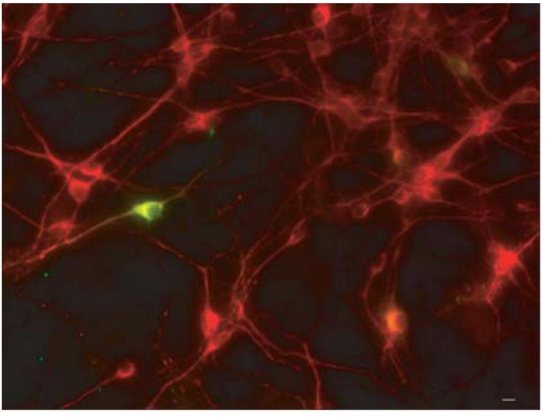
rotenone + 2 µg/ml (1)

B

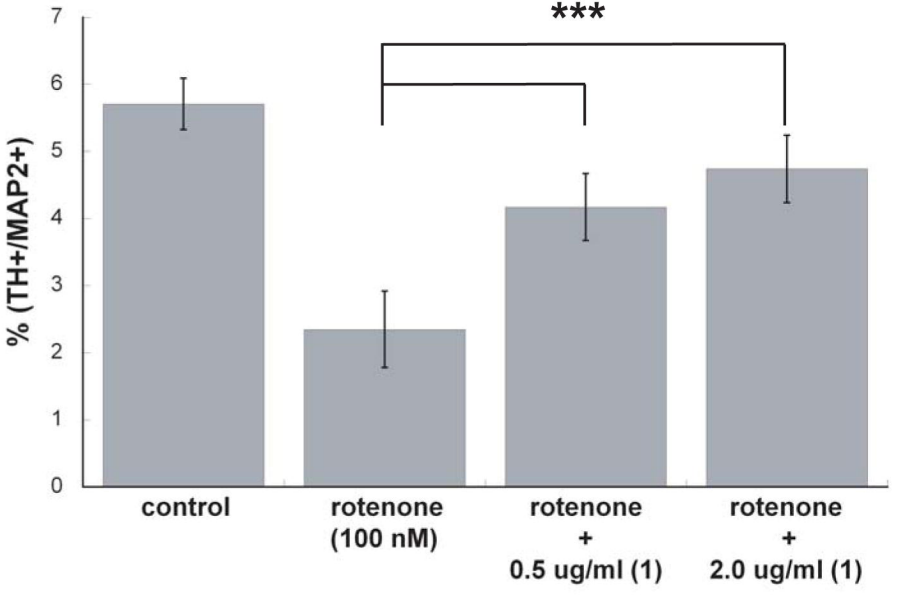
***
% (TH+/MAP2+)
0
1
2
3
4
5
6
7
control
rotenone (100 nM)
rotenone + 0.5 ug/ml (1)
rotenone + 2.0 ug/ml (1)